Precision measurements of W and Z boson production at ATLAS

Victor Solovyev

victor.solovyev@cern.ch

NRC Kurchatov Institute PNPI

On behalf of the ATLAS Collaboration

Pheno 2020

May 4-6, 2020, Pittsburgh

Introduction

Measurements of W and Z boson production at LHC provide:

- Important tests of perturbative QCD
- Information about PDFs for quarks inside the proton
- Important input to the background predictions from MC simulations used in many analyses (SM and BSM)
- Constraint on p_{T}^{W} spectrum – important for W-boson mass measurement

This talk will cover:

- p_{T} distribution of Drell-Yan lepton pairs at 13 TeV
  arXiv:1912.02844, submitted to Eur. Phys. J. C
- W and Z boson cross-sections at 2.76 TeV
  Eur. Phys. J. C 79 (2019) 901
- Z + jets cross-section at 8 TeV
  Eur. Phys. J. C 79 (2019) 847

p_{T} of Drell-Yan lepton pairs at 13 TeV

- Data: pp, $\sqrt{s} = 13$ TeV, 2015 + 2016, $\mathcal{L}_{\mathrm{int}} = 36.1\ \mathrm{fb}^{-1}$
- ee and $\mu\mu$ final states

- Selections: Single lepton trigger,
  Isolated leptons, $p_{\mathrm{T}} > 27$ GeV,
  $|\eta_e| < 2.47$, excluding $1.37 < |\eta_e| < 1.52$
  $|\eta_\mu| < 2.5$, $66 < m_{ll} < 116$ GeV

Signal:
Powheg+Pythia8

Background:
- EW, top, $\gamma\gamma$ from MC
- Multijet – data-driven

- ϕ^*_η depends only on directions of two leptons which are measured more precisely than their momenta

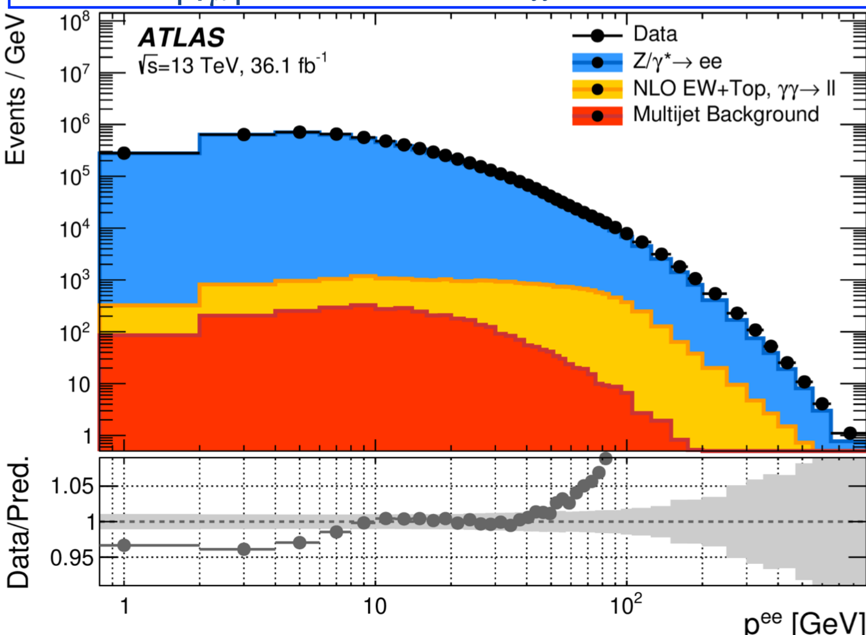

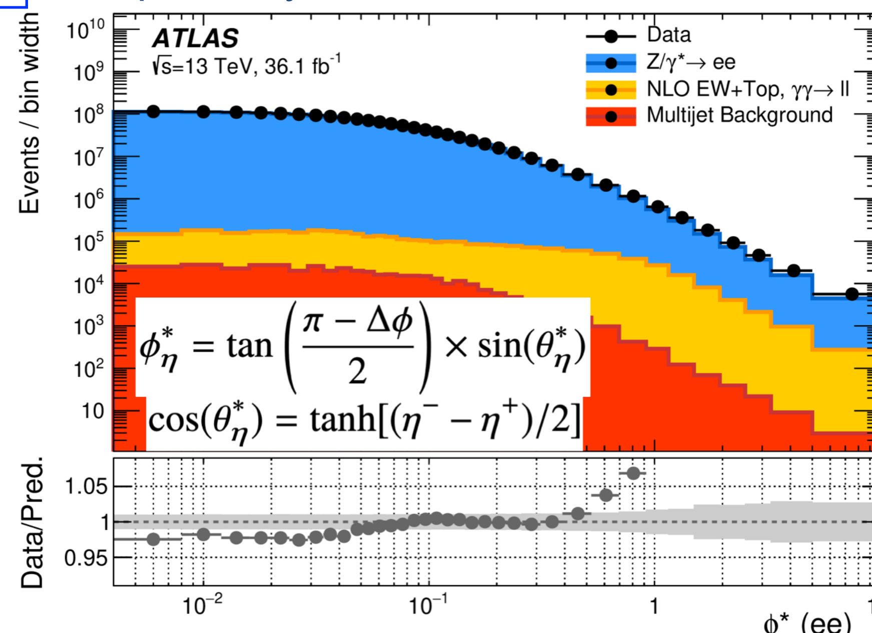

- Powheg+Pythia8 is effectively a computation at LO in α_S for large values of p_{T}^{ll} and ϕ^*_η – disagreement is expected arXiv:1912.02844

p_{T} of Drell-Yan lepton pairs at 13 TeV

- Differential distributions are corrected for detector effects and bin-to-bin migrations using an iterative Bayesian unfolding method in a fiducial volume:

$$p_{\mathrm{T}}^{l} > 27\ \mathrm{GeV},\ \ |\eta_l| < 2.5,\ \ 66 < m_{ll} < 116\ \mathrm{GeV}$$

- Uncertainties for normalized unfolded results in the electron channel:

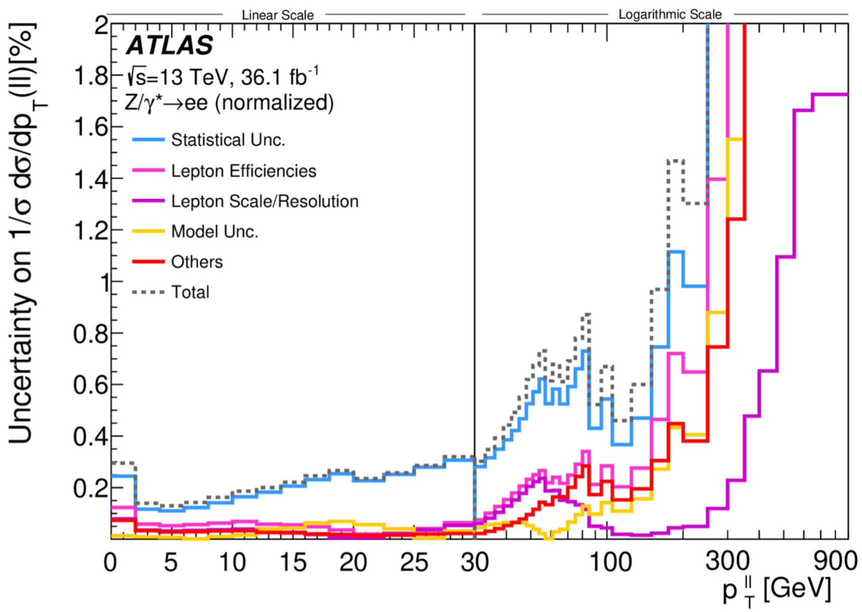

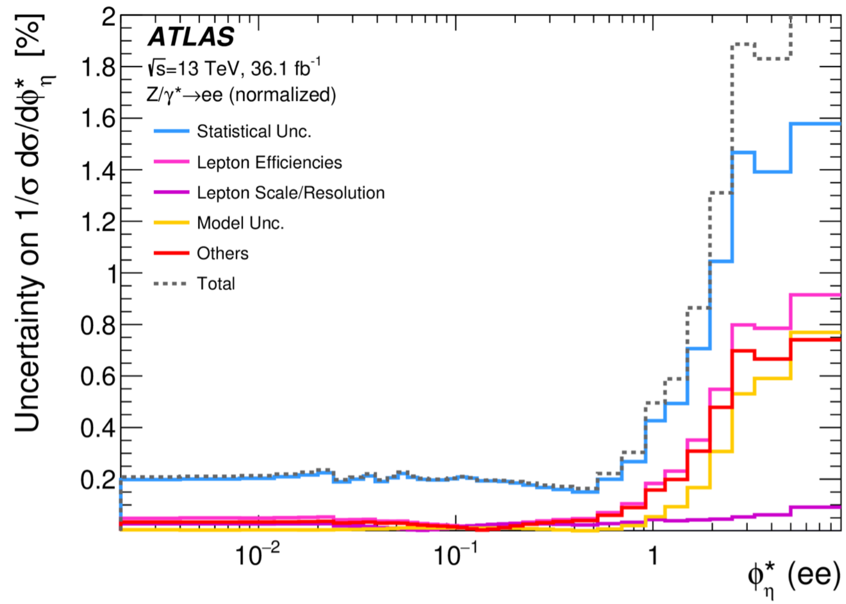

- Statistical uncertainties are dominant for both p_{T}^{ll} and ϕ_{η}^{*}
- Systematics for high values of ϕ_{η}^{*} are significantly smaller if compared to systematics for high values of p_{T}^{ll}

arXiv:1912.02844

p_{T} of Drell-Yan lepton pairs at 13 TeV

- Comparison of normalized cross-sections with different predictions

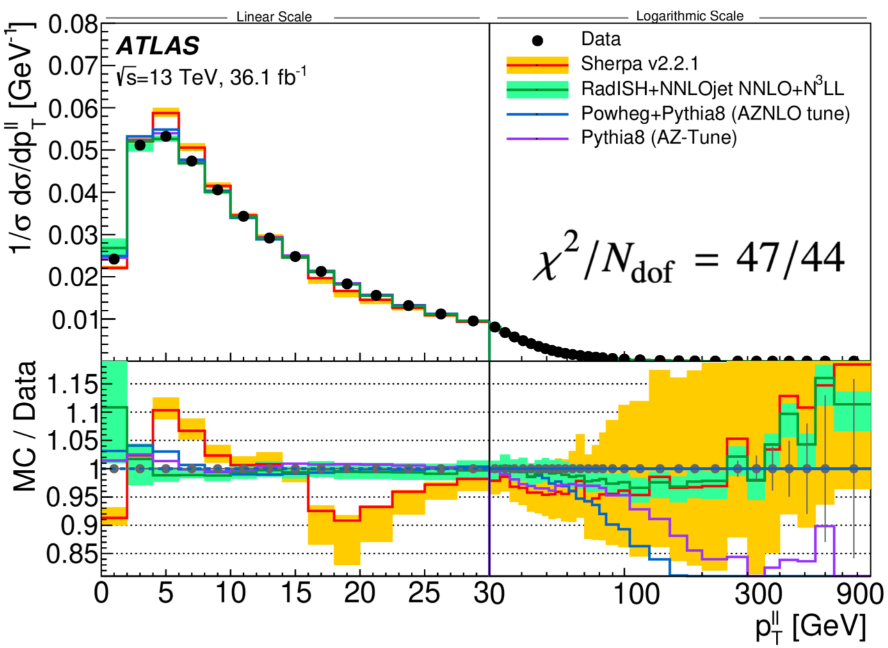

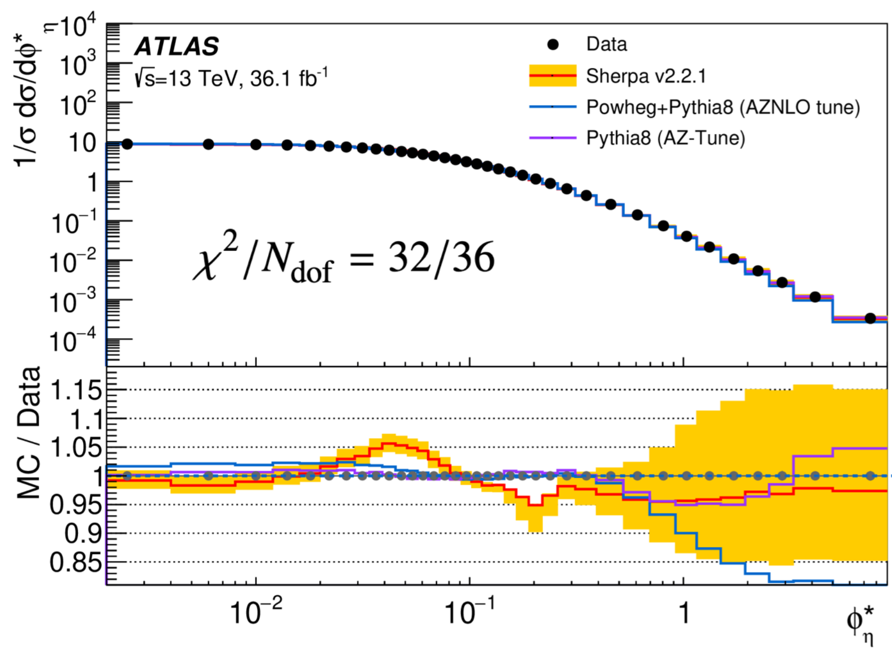

- **Pythia8** – LO ME and parton shower with AZ tune (optimized for 7 TeV data)
- **Powheg+Pythia8** – NLO ME and parton shower with AZNLO tune (optimized for 7 TeV data)
- **Sherpa 2.2.1** – NLO ME for two partons in the final state and LO ME for up to four partons
- **RadISH** – combines NNLO prediction of Z+jets production from NNLOJET with resummation of $\log(m_{ll}/p_{\mathrm{T}}^{ll})$ terms at $\mathrm{N^3LL}$ accuracy

p_{T} of Drell-Yan lepton pairs at 13 TeV

- Comparison of normalized cross-sections with different predictions

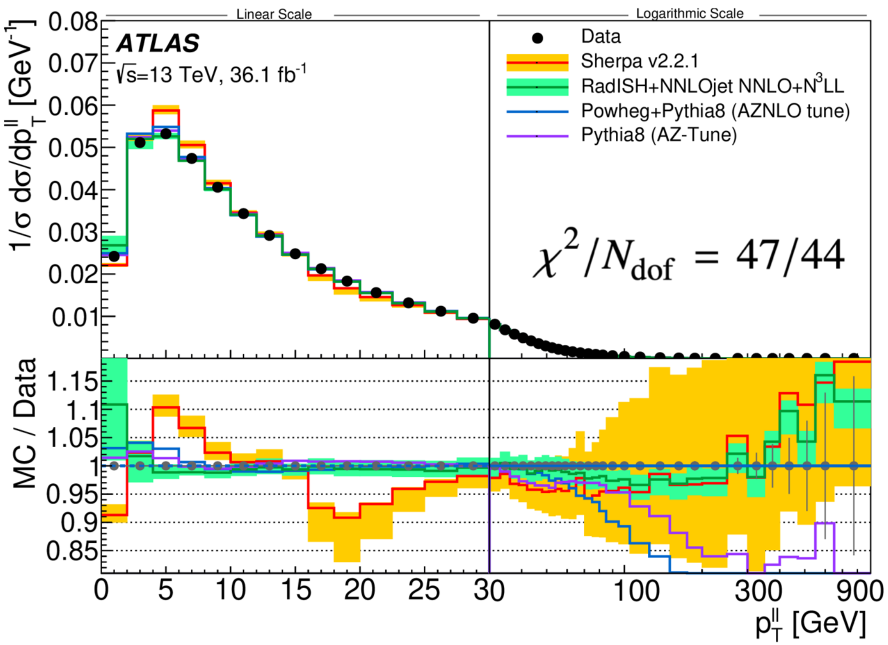

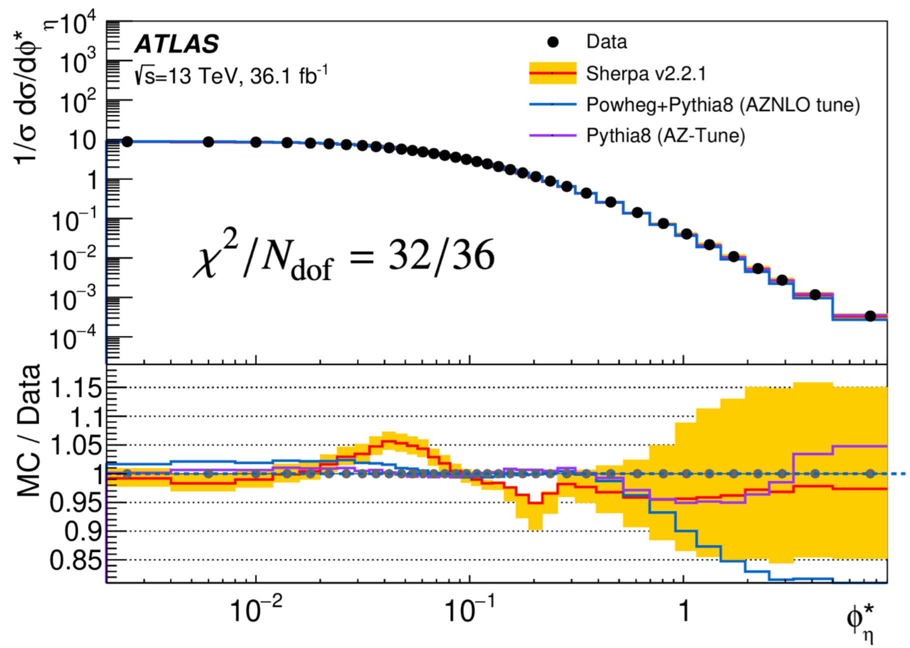

- **Pythia8** parton shower tuned to 7 TeV data describes 13 TeV data well at low p_{T}^{ll} and ϕ_η^*
- **Sherpa 2.2.1** based on merging of high-order, high-multiplicity ME – good agreement at high p_{T}^{ll}
- **RadISH+NNLOJET NNLO+N³LL** prediction agrees with data for full p_{T}^{ll} spectrum
- Relative precision is better than 0.2% for $p_{\mathrm{T}}^{ll} < 30\ \mathrm{GeV}$ – crucial information to validate and tune MC generators and to model p_{T}^{V} for the m_W measurement

Eur. Phys. J. C 79 (2019) 901

W and Z cross-sections at 2.76 TeV

- Data: pp, $\sqrt{s} = 2.76$ TeV, 2013, $\langle\mu\rangle = 0.3$, $\mathcal{L}_{\text{int}} = 4.0\ \text{pb}^{-1}$
- Measured for W^+, W^- and Z bosons
- Decay channels: $W \to l\nu$ and $Z \to ll$, where $l = e, \mu$

- Selections: Single lepton trigger, Isolated leptons,
  $p_T > 20$ GeV, $|\eta| < 2.4$,
  excl. $1.37 < |\eta| < 1.52$ for electrons

$E_T^{\text{miss}} > 25$ GeV, $m_T > 40$ GeV for W
$66 < m_{ll} < 116$ GeV for Z

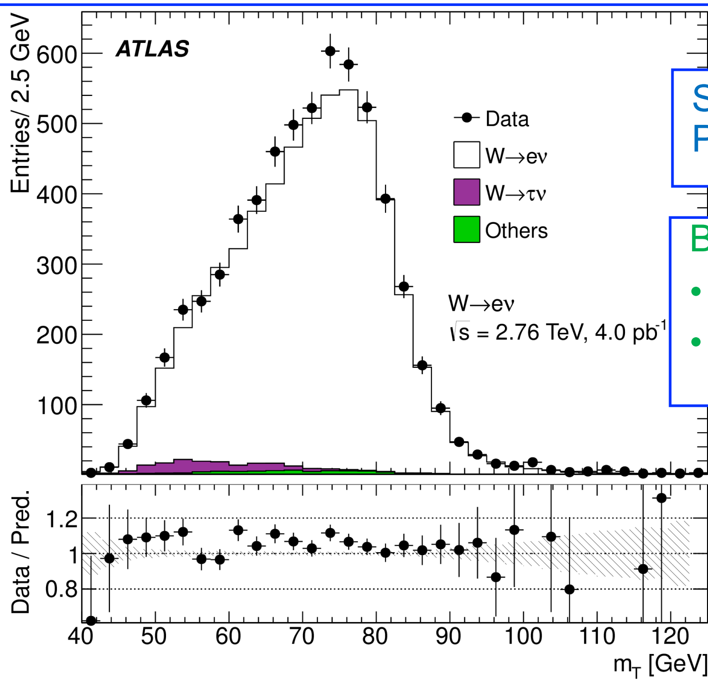

Signal:
Powheg+Pythia8

Background:
- EW and $t\bar{t}$ from MC
- Multijet – data-driven (negl. in Z selection)

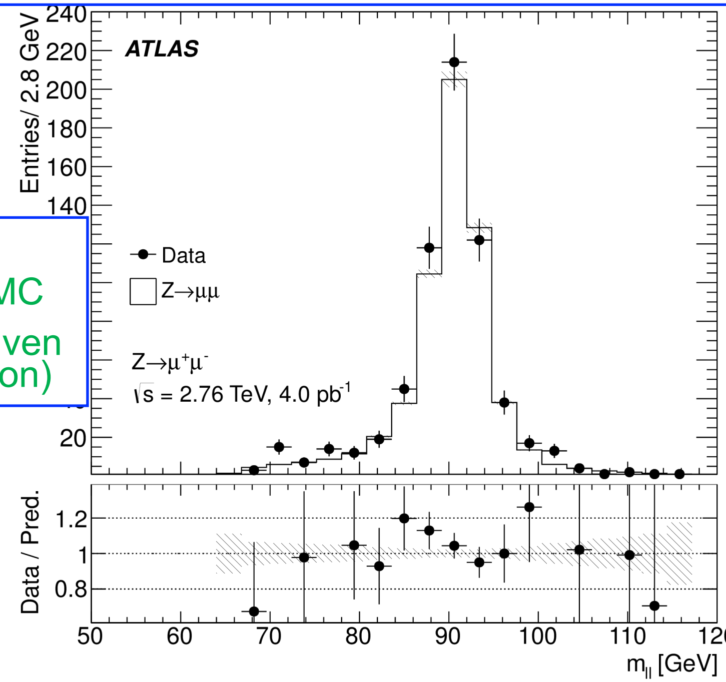

W and Z cross-sections at 2.76 TeV

- Measurements are performed at Born level within specific fiducial regions and extrapolated to full phase space

W-boson fiducial region	Z-boson fiducial region
$p_T^{\ell} > 20$ GeV	$p_T^{\ell^{+,-}} > 20$ GeV
$\lvert\eta^{\ell}\rvert < 2.4$	$\lvert\eta^{\ell^{+,-}}\rvert < 2.4$
$E_T^{miss} > 25$ GeV	$66 < m_{\ell^+\ell^-} < 116$ GeV
$m_T > 40$ GeV	

	Value ± stat. ± syst. ± lumi. (± extr.)	Value ± stat. ± syst. ± lumi. (± extr.)
	$W^+ \to \ell\nu$	$W^- \to \ell\nu$
σ_W^{fid} [pb]	$1433 \pm 16 \pm 17 \pm 44$	$798 \pm 12 \pm 10 \pm 25$
σ_W^{tot} [pb]	$2312 \pm 26 \pm 27 \pm 72 (\pm 30)$	$1399 \pm 21 \pm 17 \pm 43 (\pm 21)$
	$W \to \ell\nu$	
σ_W^{fid} [pb]	$2231 \pm 20 \pm 26 \pm 69$	
σ_W^{tot} [pb]	$3711 \pm 34 \pm 43 \pm 115 (\pm 51)$	
	$Z \to \ell\ell$	
σ_Z^{fid} [pb]	$203.7 \pm 6.2 \pm 3.2 \pm 6.3$	
σ_Z^{tot} [pb]	$323.4 \pm 9.8 \pm 5.0 \pm 10.0 (\pm 5.5)$	

- Ratios of cross-sections have significantly reduced systematic uncertainties due to cancellation of correlated uncertainties:

$$R_{W/Z} = 10.95 \pm 0.35\,(\text{stat.}) \pm 0.10\,(\text{syst.});$$

$$R_{W^+/W^-} = 1.797 \pm 0.034\,(\text{stat.}) \pm 0.009\,(\text{syst.}).$$

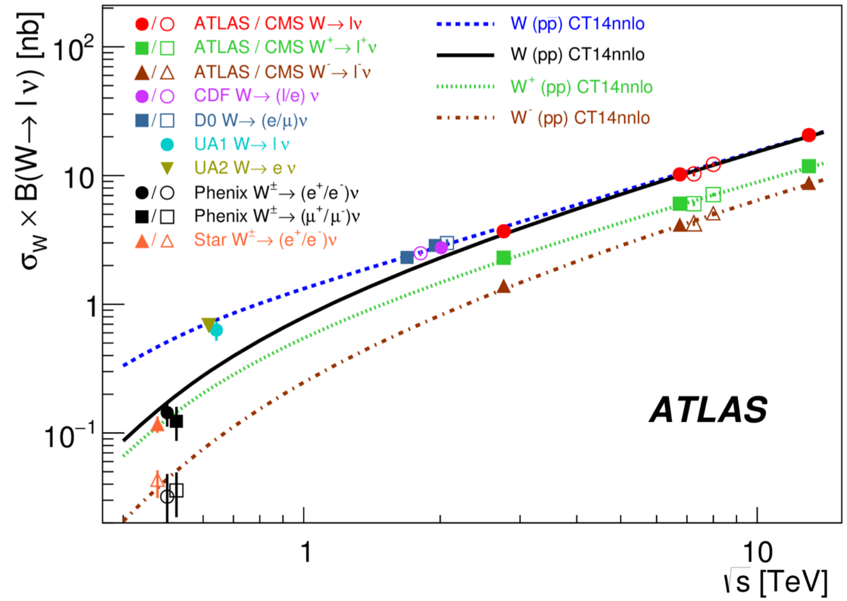

Eur. Phys. J. C 79 (2019) 901

W and Z cross-sections at 2.76 TeV

- Comparison of measured fiducial cross-sections and their ratios with predictions from various PDF sets

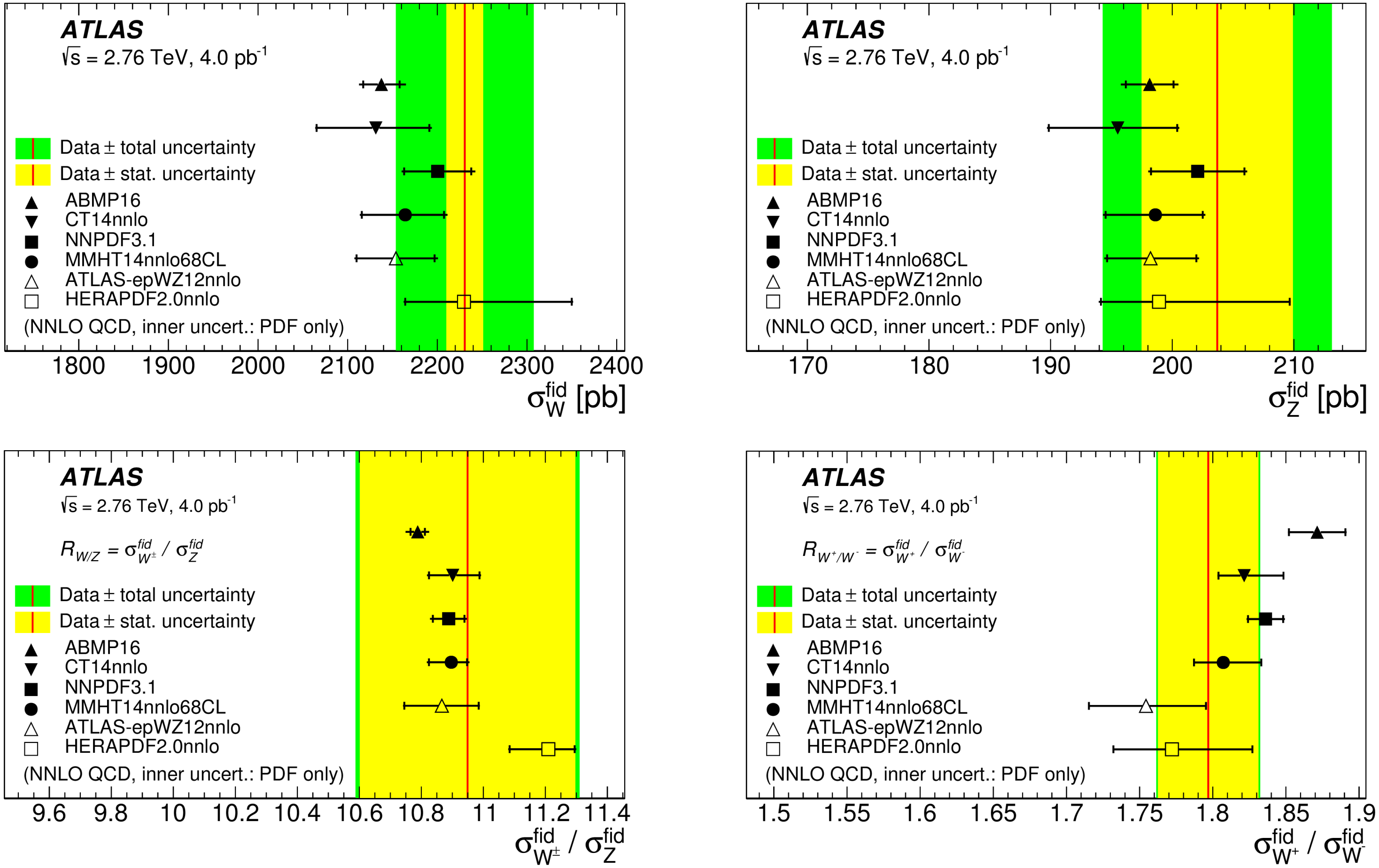

- Measurements and SM predictions are mostly in good agreement

Eur. Phys. J. C 79 (2019) 847

Z + jets cross-section at 8 TeV

- Data: pp, $\sqrt{s} = 8$ TeV, 2012, $\mathcal{L}_{\text{int}} = 19.9\ \text{fb}^{-1}$
- $Z \to ee$ decay channel

Signal:
- Sherpa v1.4 norm. to NNLO – main sample
- Alpgen+Pythia6 norm. to NNLO – data compar.

- Selections: Dielectron trigger,
  $p_T^e > 20$ GeV, $|\eta_e| < 2.47$
  excl. $1.37 < |\eta_e| < 1.52$
  $66 < m_{ee} < 116$ GeV
  $p_T^{\text{jet}} > 25$ GeV
  $|\eta_{\text{jet}}| < 3.4$

Background:
- Top and EW – from MC
- Multijet, W+jets – data-driven

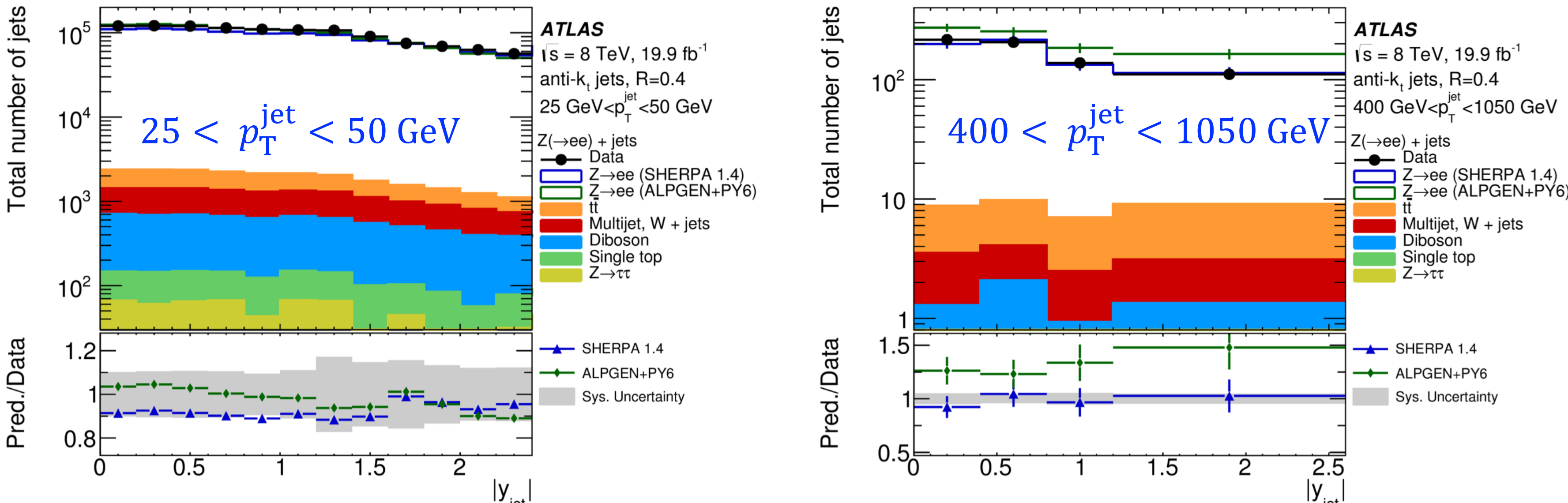

- Measurements are performed in six p_T^{jet} bins in range from 25 to 1050 GeV as function of $|y_{\text{jet}}|$
- Reconstructed spectra are then corrected for detector effects using iterative Bayesian unfolding

Eur. Phys. J. C 79 (2019) 847

Z + jets cross-section at 8 TeV

- Double-differential cross-section as function of $|y_{\mathrm{jet}}|$ and $p_{\mathrm{T}}^{\mathrm{jet}}$ is measured

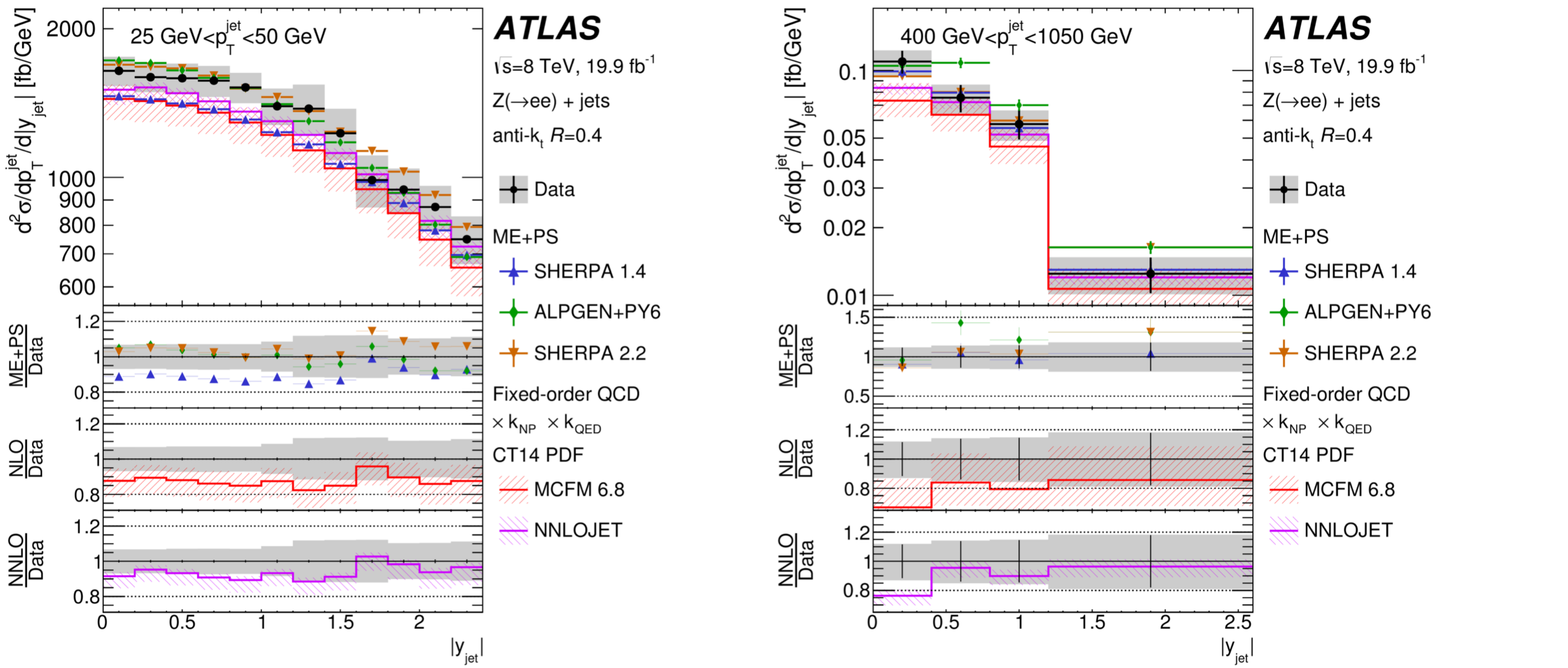

- **Sherpa 1.4:** lower than data by 10% for $p_{\mathrm{T}}^{\mathrm{jet}} < 200\ \mathrm{GeV}$. Good agreement for higher $p_{\mathrm{T}}^{\mathrm{jet}}$
- **Alpgen+Pythia6:** agrees with data for $p_{\mathrm{T}}^{\mathrm{jet}} < 100\ \mathrm{GeV}$. Exceeds data up to 20% for higher $p_{\mathrm{T}}^{\mathrm{jet}}$
- **Sherpa 2.2:** good agreement in all bins
- **MCFM (NLO):** lower than data by 5-10%
- **NNLOJET (NNLO):** good agreement in all bins

Summary

- **p_T distribution of Drell-Yan lepton pairs at 13 TeV**
  - Cross-sections differential in the transverse momentum of Z boson were measured covering up to TeV-range
  - Results provide crucial information to validate and tune MC event generators and will constrain models of vector-boson production in future measurements of the W boson mass

- **W and Z boson cross-sections at 2.76 TeV**
  - Measured for W^+, W^- and Z bosons
  - Measured cross-sections and cross-section ratios are in good agreement with theoretical calculations based on NNLO QCD

- **Z + jets cross-section at 8 TeV**
  - Double-differential cross-section was measured as a function of $|y_{\mathrm{jet}}|$ and p_T^{jet}
  - Good agreement with MC generator predictions and with NLO and NNLO calculations was observed

Backup

p_{T} of Drell-Yan lepton pairs at 13 TeV

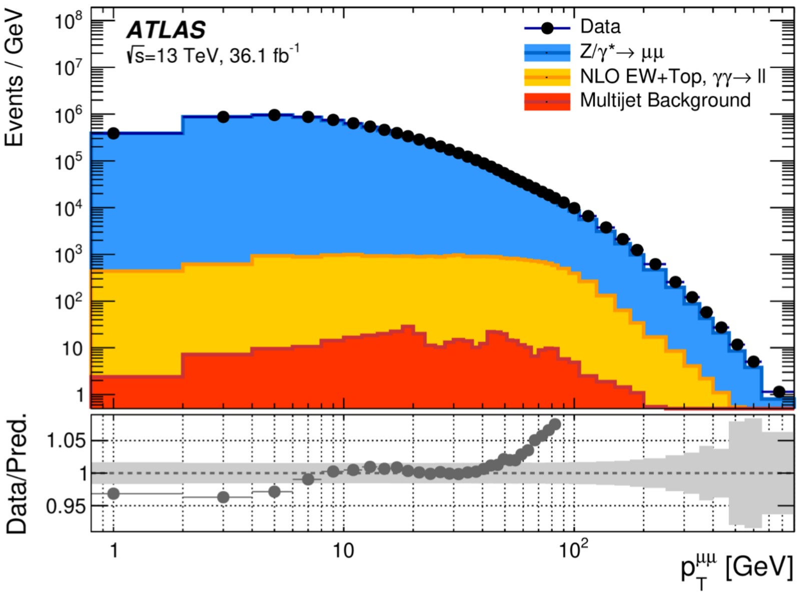

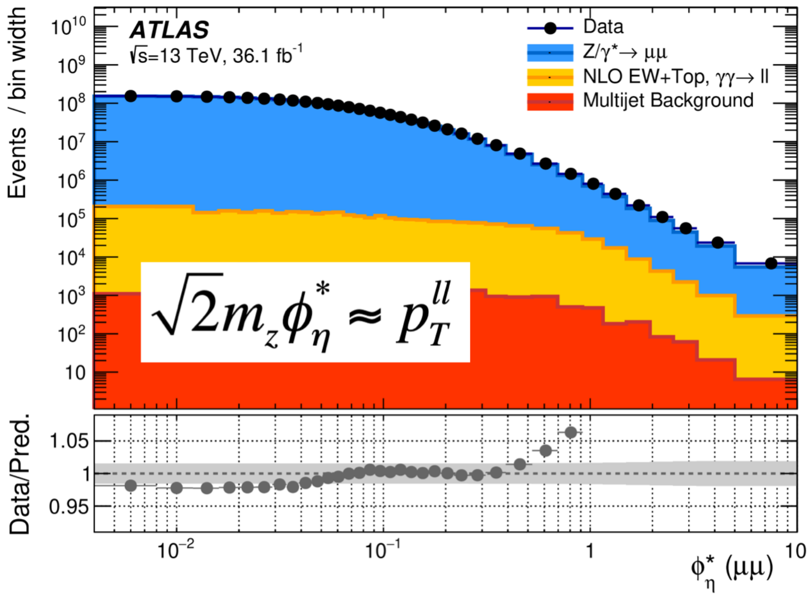

	$Z/\gamma^* \to ee$	$Z/\gamma^* \to \mu\mu$
Two reconstructed leptons within fiducial volume	13 649 239	18 162 641
Electroweak background ($Z \to \tau\tau$, WW, WZ, ZZ)	40 000 ± 2000	39 000 ± 2000
Photon-induced background	2900 ± 140	4100 ± 200
Top-quark background	38 000 ± 1900	45 400 ± 2200
Multijet background	8500 ± 4900	1000 ± 200

p_{T} of Drell-Yan lepton pairs at 13 TeV

- Production cross-sections are measured in the fiducial volumes at Born and dressed levels

$$\sigma^{\mathrm{fid}}_{Z/\gamma^*\to\ell\ell} = \frac{N_{\mathrm{Data}} - N_{\mathrm{Bkg}}}{C_Z \cdot L}$$

	Electron channel		Muon channel	
	Born	Dressed	Born	Dressed
C_Z	0.509 ± 0.005	0.522 ± 0.005	0.685 ± 0.011	0.702 ± 0.011
Trigger efficiencies	± 0.0004		± 0.0004	
Identification & reconstruction efficiencies	± 0.0049		± 0.0102	
Isolation efficiencies	± 0.0009		± 0.0029	
Energy/momentum scale and resolution	± 0.0014		± 0.0010	
Pile-up	± 0.0011		± 0.0019	
Model uncertainties	± 0.0001		± 0.0001	

Channel	Measured cross-section $\times \mathcal{B}(Z/\gamma^* \to \ell\ell)$ (value $\pm$ stat. $\pm$ syst. $\pm$ lumi.)	Predicted cross-section $\times \mathcal{B}(Z/\gamma^* \to \ell\ell)$ (value $\pm$ PDF $\pm$ α_S $\pm$ scale $\pm$ intrinsic)
$Z/\gamma^* \to ee$	$738.3 \pm 0.2 \pm 7.7 \pm 15.5$ pb	
$Z/\gamma^* \to \mu\mu$	$731.7 \pm 0.2 \pm 11.3 \pm 15.3$ pb	
$Z/\gamma^* \to \ell\ell$	$736.2 \pm 0.2 \pm 6.4 \pm 15.5$ pb	$703^{+19}_{-24}\,^{+6}_{-8}\,^{+4}_{-6}\,^{+5}_{-5}$ pb **[STDM-2016-02]**

p_T of Drell-Yan lepton pairs at 13 TeV

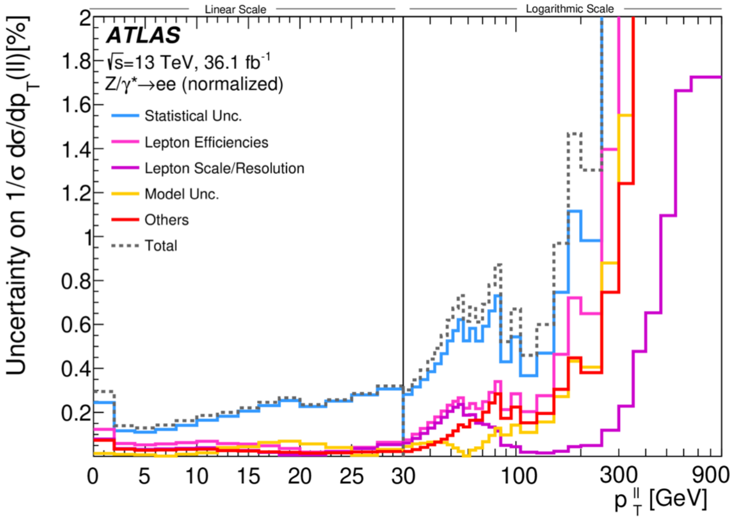

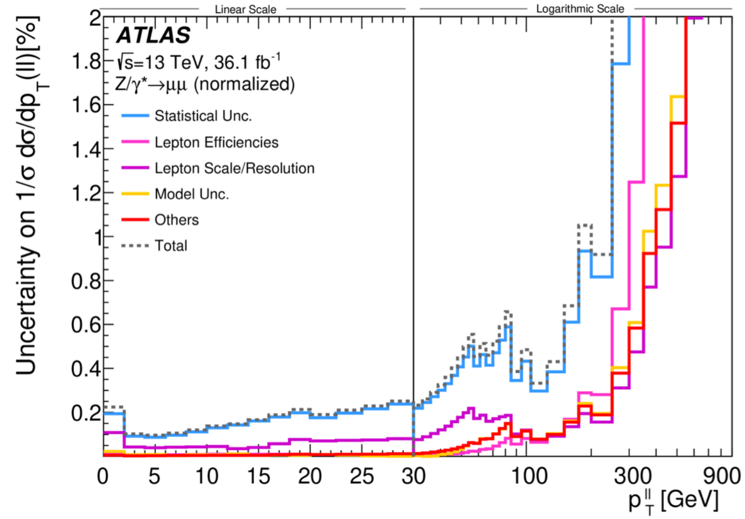

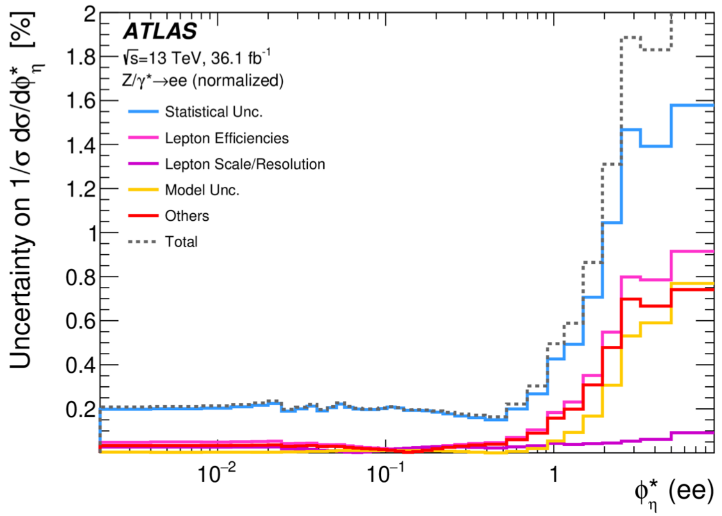

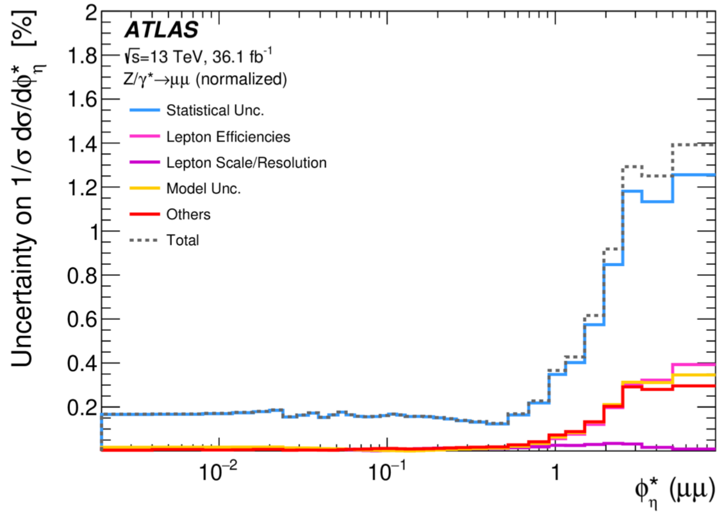

p_{T} of Drell-Yan lepton pairs at 13 TeV

- Differential distributions are corrected for detector effects using an iterative Bayesian unfolding method with 4 iterations
- Two channels are combined using χ^2 minimization, following the best linear unbiased estimator prescription

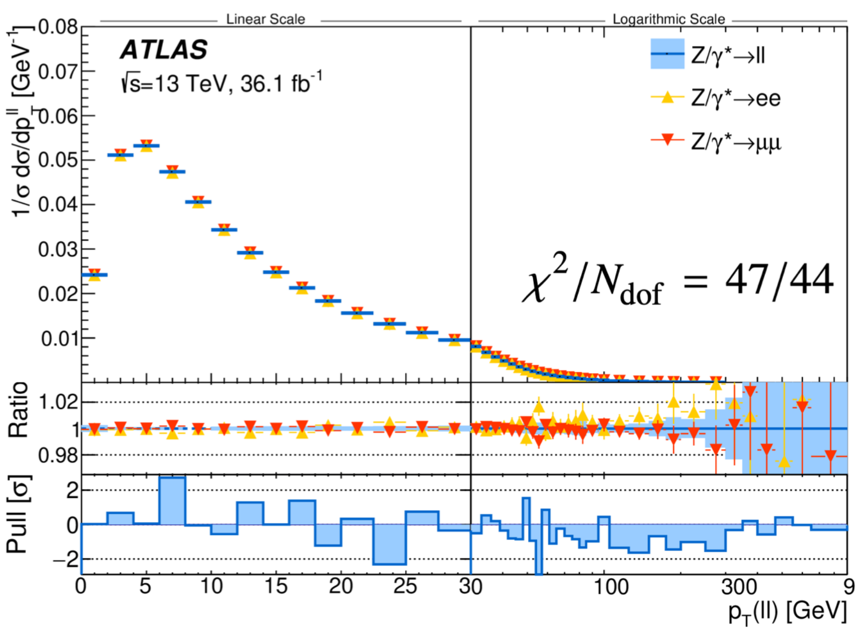

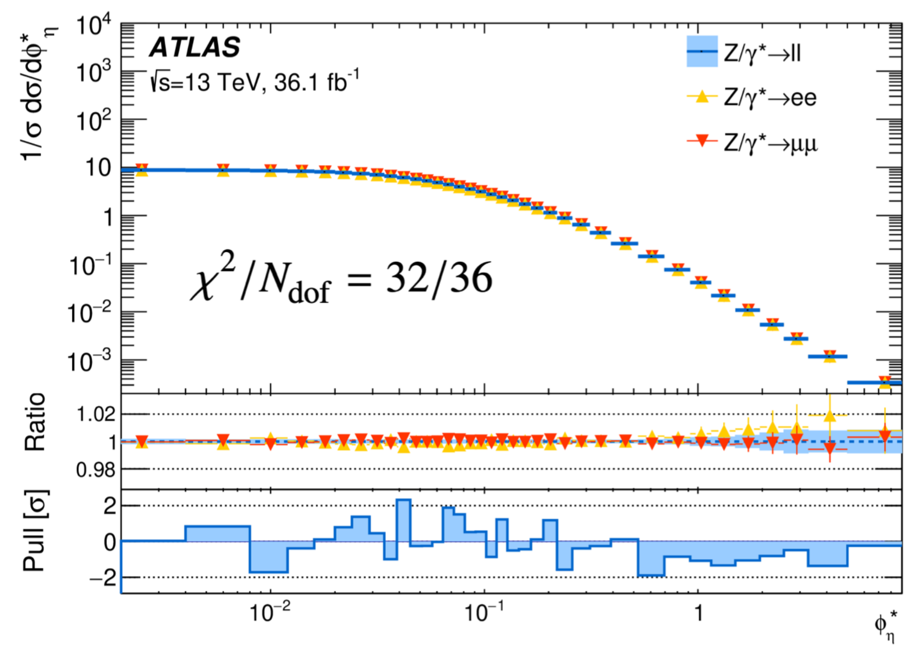

p_{T} of Drell-Yan lepton pairs at 13 TeV

- Differential distributions are corrected for detector effects using an iterative Bayesian unfolding method in a fiducial volume: $p_{\mathrm{T}}^{l} > 27\ \mathrm{GeV}, |\eta_l| < 2.5, 66 < m_{ll} < 116\ \mathrm{GeV}$

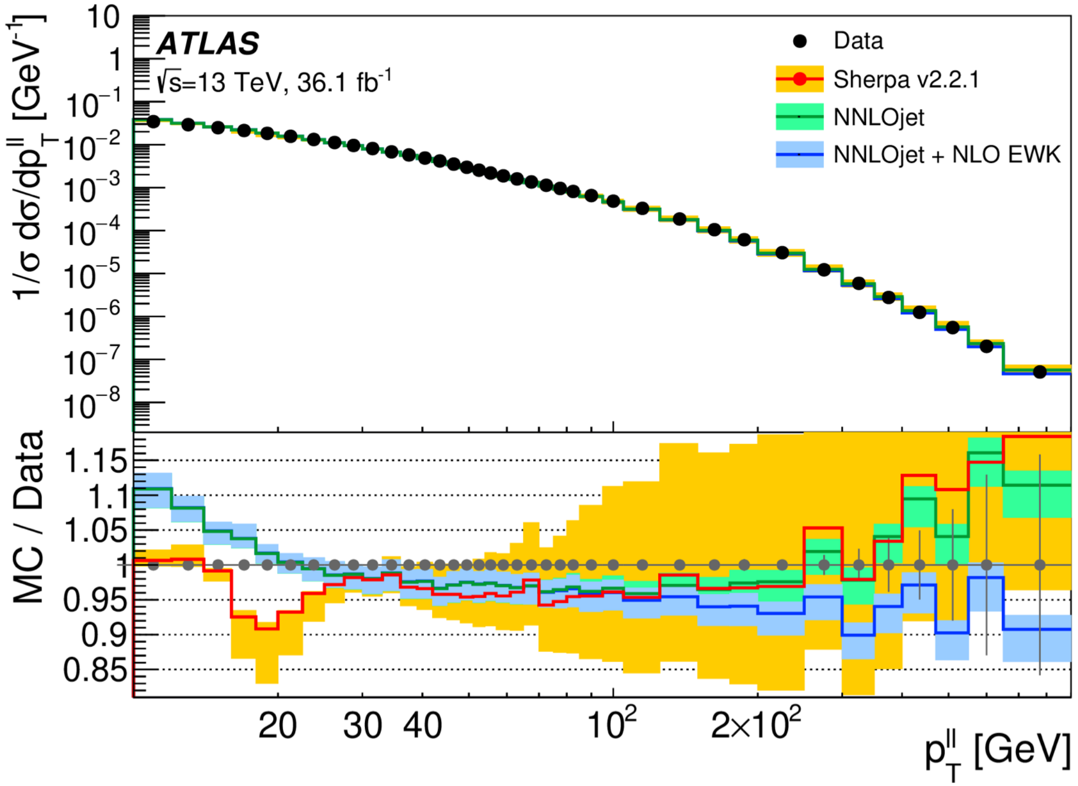

- The fixed-order NNLOjet prediction with and without NLO EW effects describes the data well for high p_{T}^{ll}

W and Z cross-sections at 2.76 TeV

- Measurements are performed at Born level within specific fiducial regions and extrapolated to full phase space

W-boson fiducial region	Z-boson fiducial region
$p_{\mathrm{T}}^{\ell} > 20$ GeV	$p_{\mathrm{T}}^{\ell^{+,-}} > 20$ GeV
$\lvert\eta^{\ell}\rvert < 2.4$	$\lvert\eta^{\ell^{+,-}}\rvert < 2.4$
$E_{\mathrm{T}}^{\mathrm{miss}} > 25$ GeV	$66 < m_{\ell^+\ell^-} < 116$ GeV
$m_{\mathrm{T}} > 40$ GeV	

	Value ± stat. ± syst. ± lumi. (± extr.)	Value ± stat. ± syst. ± lumi. (± extr.)
	$W^+ \to \ell\nu$	$W^- \to \ell\nu$
σ_W^{fid} [pb]	1433 ± 16 ± 17 ± 44	798 ± 12 ± 10 ± 25
σ_W^{tot} [pb]	2312 ± 26 ± 27 ± 72 (±30)	1399 ± 21 ± 17 ± 43 (±21)
	$W \to \ell\nu$	
σ_W^{fid} [pb]	2231 ± 20 ± 26 ± 69	
σ_W^{tot} [pb]	3711 ± 34 ± 43 ± 115 (±51)	
	$Z \to \ell\ell$	
σ_Z^{fid} [pb]	203.7 ± 6.2 ± 3.2 ± 6.3	
σ_Z^{tot} [pb]	323.4 ± 9.8 ± 5.0 ± 10.0 (±5.5)	

- Ratios of cross-sections have significantly reduced systematic uncertainties due to cancellation of correlated uncertainties

Sensitive to:

$$R_{W/Z} = 10.95 \pm 0.35\,(\text{stat.}) \pm 0.10\,(\text{syst.});$$ ← *s* quark distribution

$$R_{W^+/W^-} = 1.797 \pm 0.034\,(\text{stat.}) \pm 0.009\,(\text{syst.}).$$ ← *u* and *d* valence quark distributions

W and Z cross-sections at 2.76 TeV

- Comparison of predicted and measured cross-sections at different centre-of-mass energies for pp and $p\bar{p}$ collisions

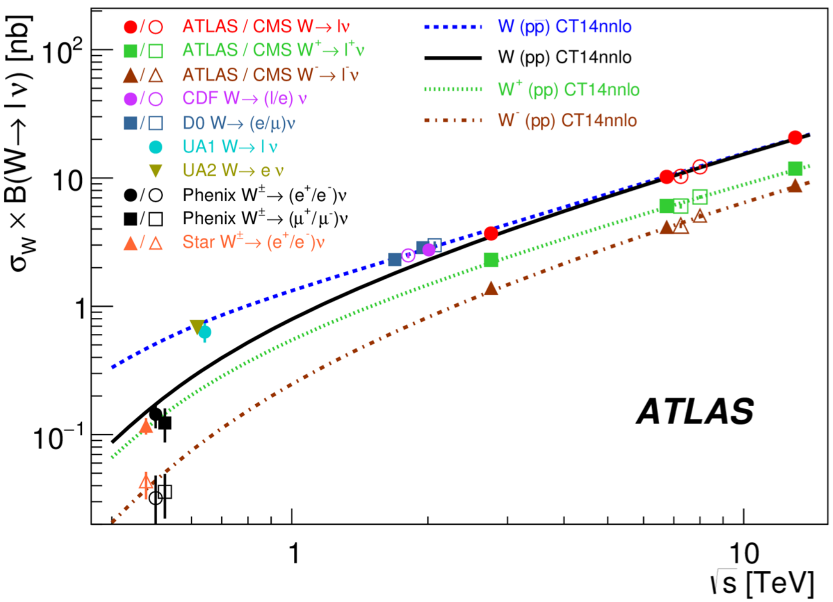

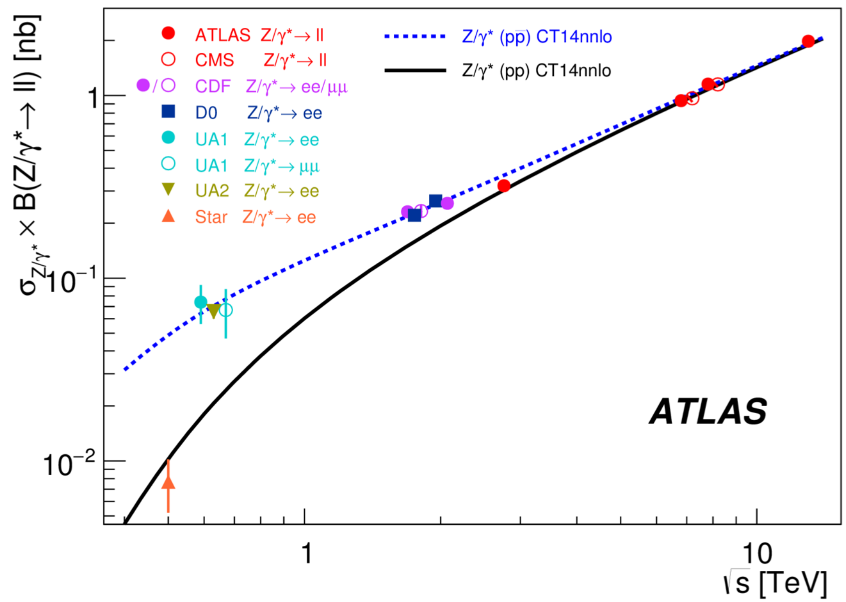

$$\sigma^{\text{fid}}_{W,Z\to\ell\nu,\ell\ell} = \frac{N^{\text{sig}}_{W,Z}}{C_{W,Z}\cdot\mathcal{L}_{\text{int}}}$$

$$\sigma^{\text{tot}}_{W,Z\to\ell\nu,\ell\ell} \equiv \sigma^{\text{tot}} \times B(W,Z\to\ell\nu,\ell\ell) = \frac{N^{\text{sig}}_{W,Z}}{A_{W,Z}\cdot C_{W,Z}\cdot\mathcal{L}_{\text{int}}}.$$

W and Z cross-sections at 2.76 TeV

$\delta C/C[\%]$	$W^+ \to e^+\nu$	$W^- \to e^-\nu$	$Z \to e^+e^-$	$W^+ \to \mu^+\nu$	$W^- \to \mu^-\nu$	$Z \to \mu^+\mu^-$
Lepton trigger	0.14	0.13	< 0.01	1.07	1.07	0.03
Lepton reconstr. and ident.	2.31	2.33	4.55	0.30	0.32	0.62
Lepton isolation	0.71	0.71	1.41	0.51	0.51	1.01
Lepton scale and resolution	0.44	0.43	0.34	0.05	0.05	0.04
Recoil scale and resolution	0.25	0.20	–	0.22	0.22	–
PDF	0.22	0.29	0.11	0.11	0.20	0.06
MC statistical uncertainty	0.24	0.31	0.30	0.24	0.34	0.43
Total	2.5	2.5	4.8	1.3	1.3	1.3

Measurement Channel	Observed candidates	Background (EW + top)	Background (Multijet)	Background-subtracted data N_W^{sig}
$W^+ \to e^+\nu$	3914	108 ± 6	30 ± 11	3776 ± 63 ± 12
$W^- \to e^-\bar{\nu}$	2209	74.2 ± 3.3	30 ± 11	2105 ± 47 ± 12
$W^+ \to \mu^+\nu$	4365	152 ± 7	2.5 ± 1.9	4210 ± 66 ± 7
$W^- \to \mu^-\bar{\nu}$	2460	108 ± 4	2.5 ± 1.9	2350 ± 50 ± 5
$Z \to e^+e^-$	430	1.3 ± 0.0	–	428.7 ± 20.7 ± 0.0
$Z \to \mu^+\mu^-$	646	1.6 ± 0.1	–	644.4 ± 25.4 ± 0.1

W and Z cross-sections at 2.76 TeV

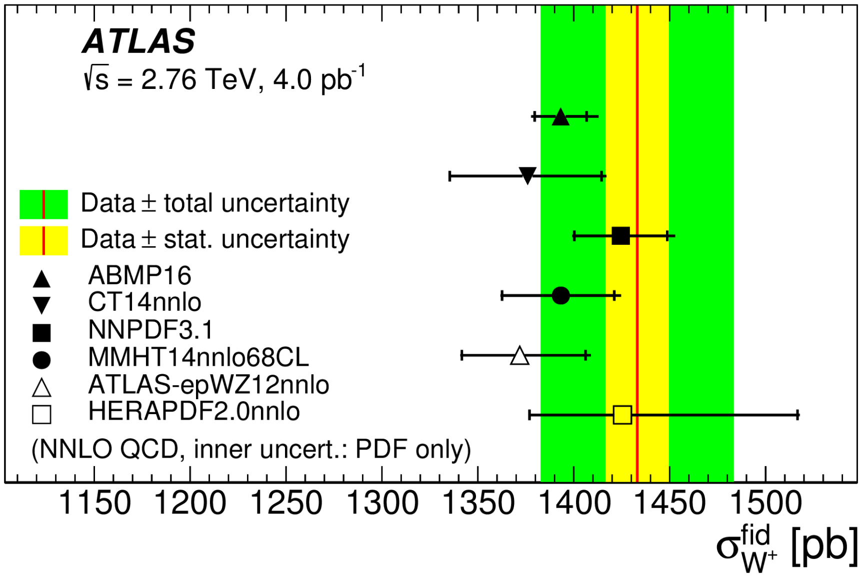

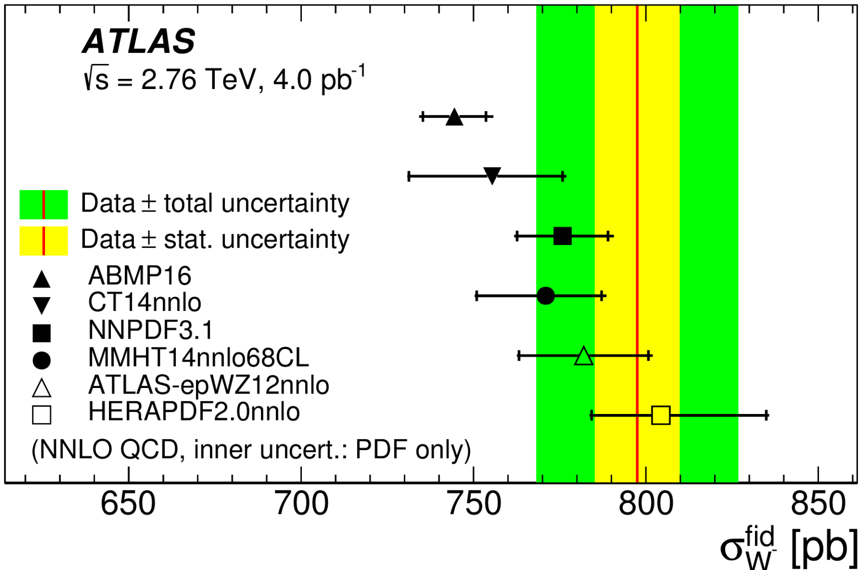

Charge asymmetry:

$$A_\ell = \frac{\sigma^{\text{fid}}_{W^+} - \sigma^{\text{fid}}_{W^-}}{\sigma^{\text{fid}}_{W^+} + \sigma^{\text{fid}}_{W^-}}$$

$$= 0.285 \pm 0.009(\text{stat.}) \pm 0.002(\text{syst.})$$

Test of lepton universality:

$$R_{W^+} = \frac{\sigma^{\text{fid}}_{W^+\to e^+\nu}}{\sigma^{\text{fid}}_{W^+\to \mu^+\nu}} = 0.985 \pm 0.023\ (\text{stat.})\ \pm 0.028\ (\text{syst.})$$

$$R_{W^-} = \frac{\sigma^{\text{fid}}_{W^-\to e^-\bar{\nu}}}{\sigma^{\text{fid}}_{W^-\to \mu^-\bar{\nu}}} = 0.988 \pm 0.030\ (\text{stat.})\ \pm 0.028\ (\text{syst.})$$

$$R_{W} = \frac{\sigma^{\text{fid}}_{W\to e\nu}}{\sigma^{\text{fid}}_{W\to \mu\nu}} = 0.986 \pm 0.018\ (\text{stat.})\ \pm 0.028\ (\text{syst.})$$

$$R_{Z} = \frac{\sigma^{\text{fid}}_{Z\to e^+e^-}}{\sigma^{\text{fid}}_{Z\to \mu^+\mu^-}} = 0.96 \pm 0.06\ (\text{stat.})\ \pm 0.05\ (\text{syst.})$$

Z + jets cross-section at 8 TeV

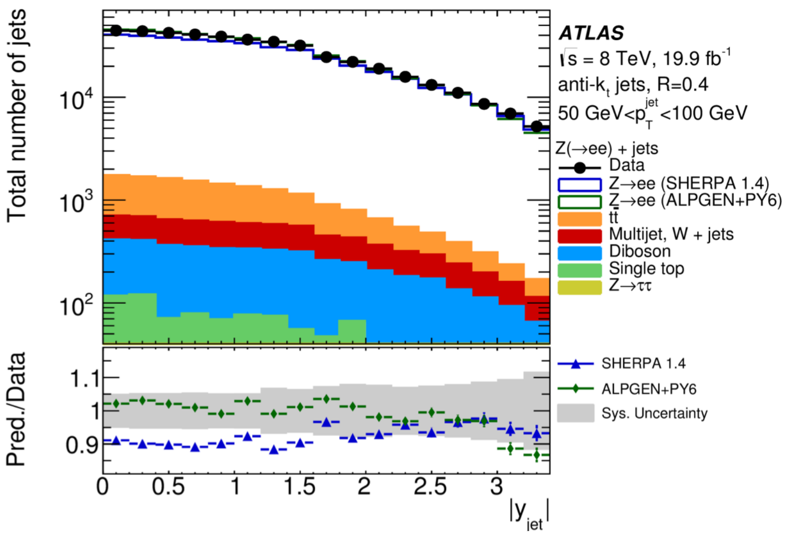

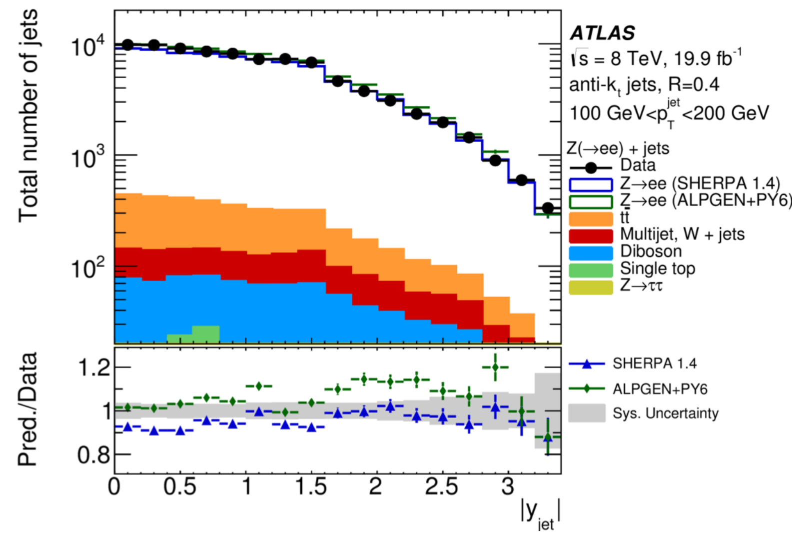

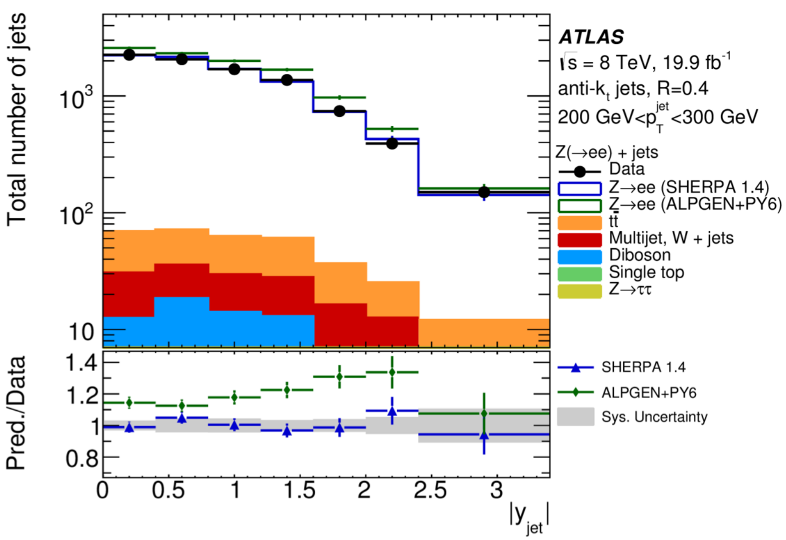

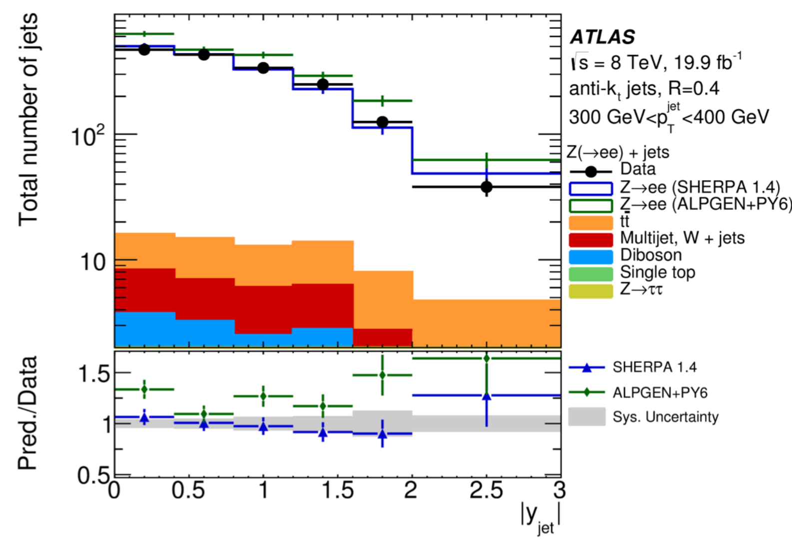

Z + jets cross-section at 8 TeV

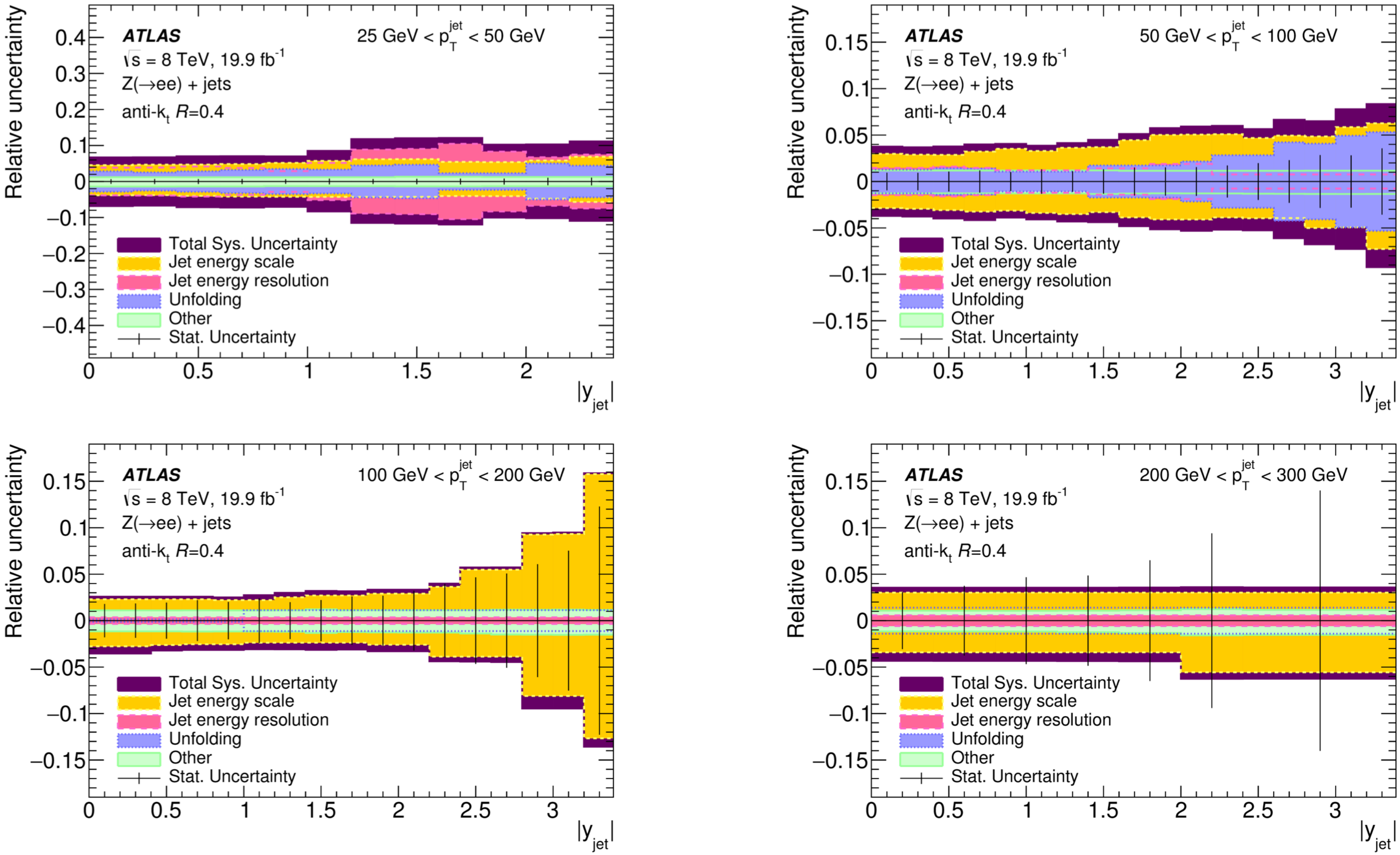

Z + jets cross-section at 8 TeV

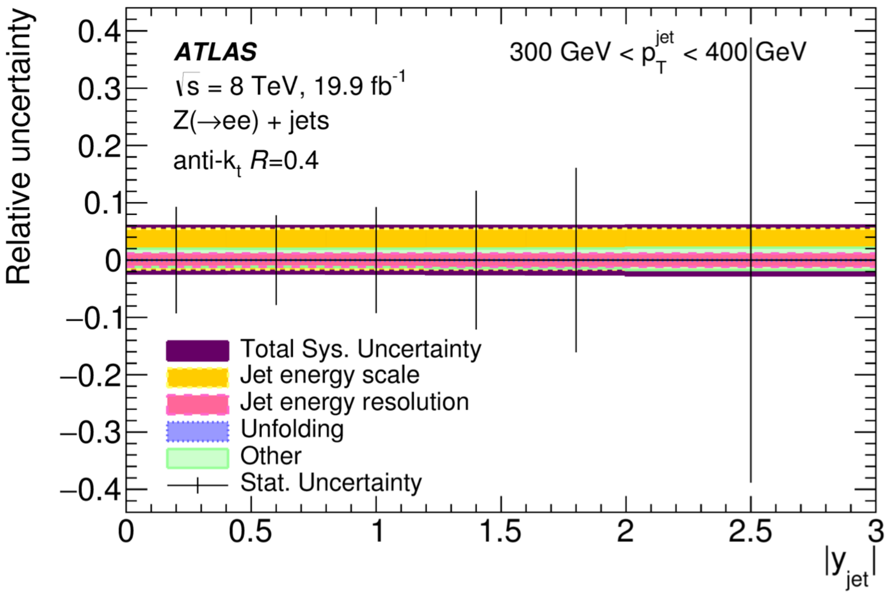

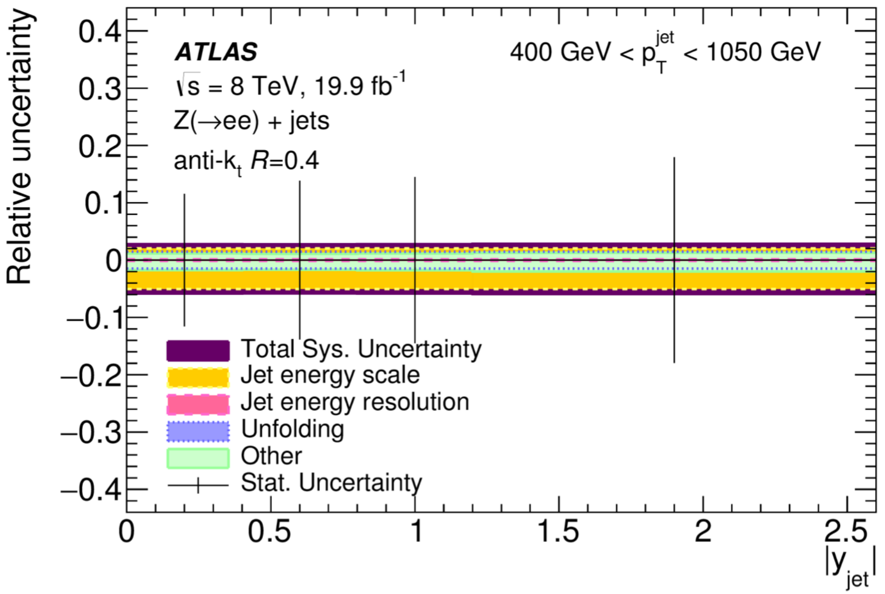

Eur. Phys. J. C 79 (2019) 847

Z + jets cross-section at 8 TeV

- Double-differential cross-section as function of $|y_{\text{jet}}|$ and $p_{\text{T}}^{\text{jet}}$ is measured

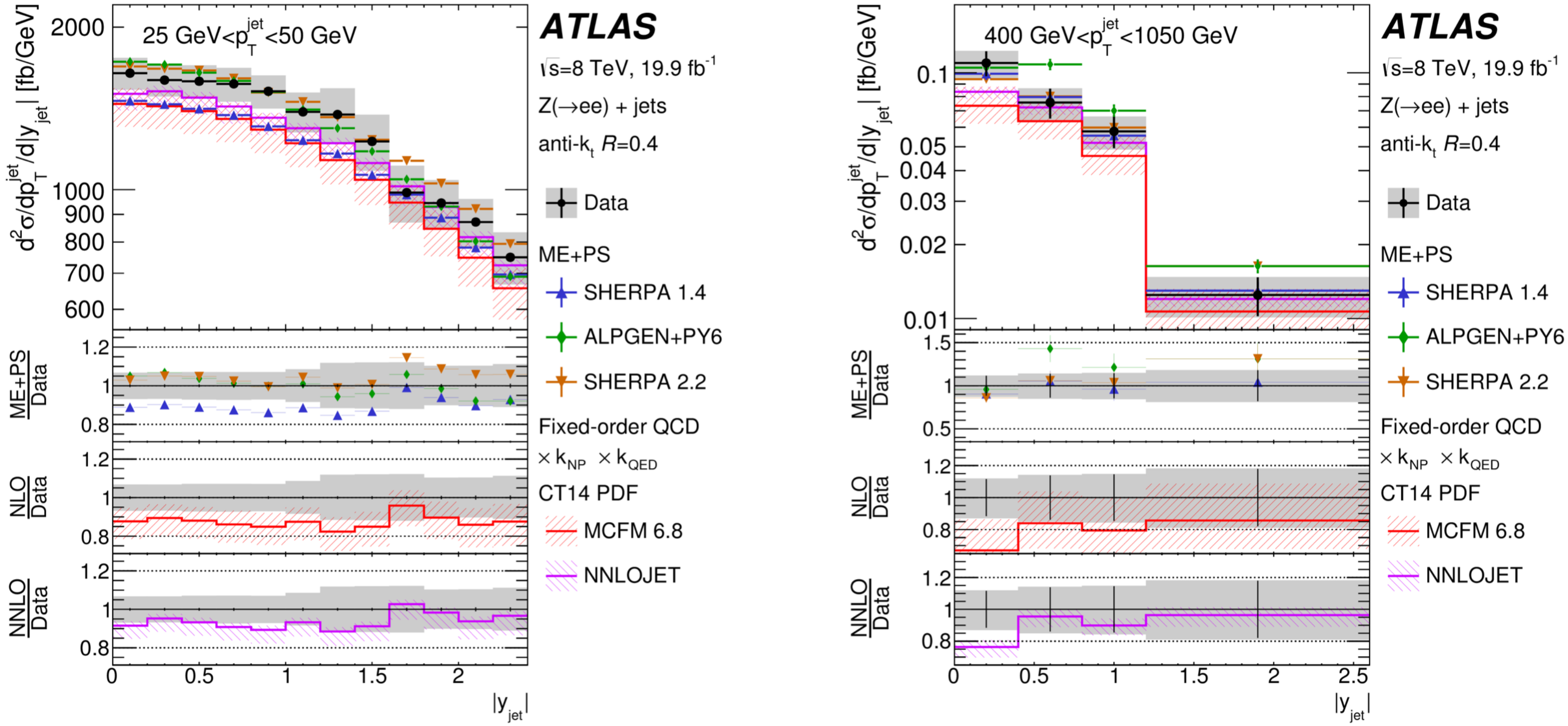

- **Sherpa 1.4:** NLO ME for inclusive Z boson production and LO ME for up to five partons
- **Alpgen+Pythia6:** up to five partons in the final state at LO
- **Sherpa 2.2:** NLO ME for two partons in the final state and LO ME for up to four partons

Z + jets cross-section at 8 TeV

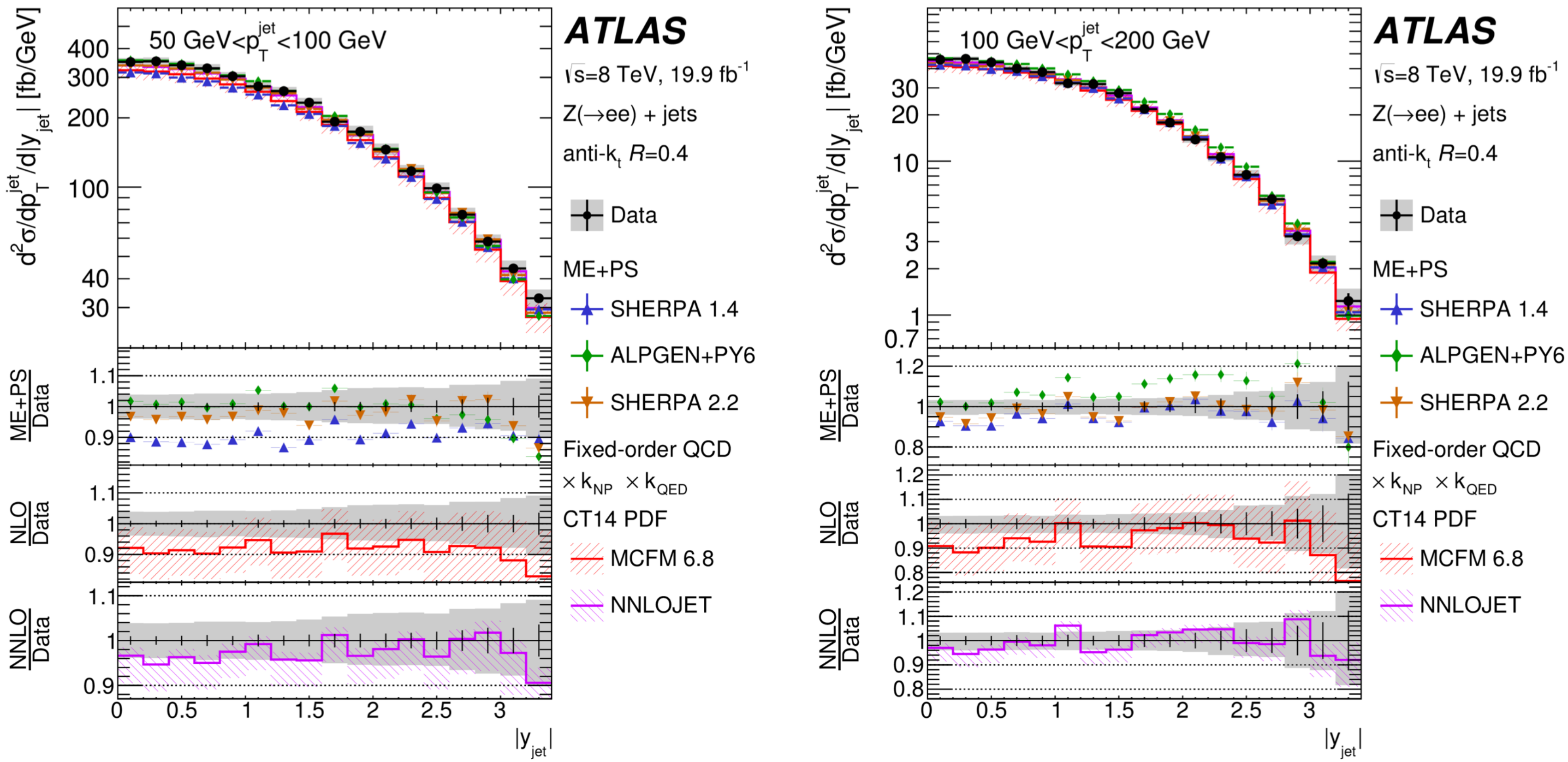

Z + jets cross-section at 8 TeV

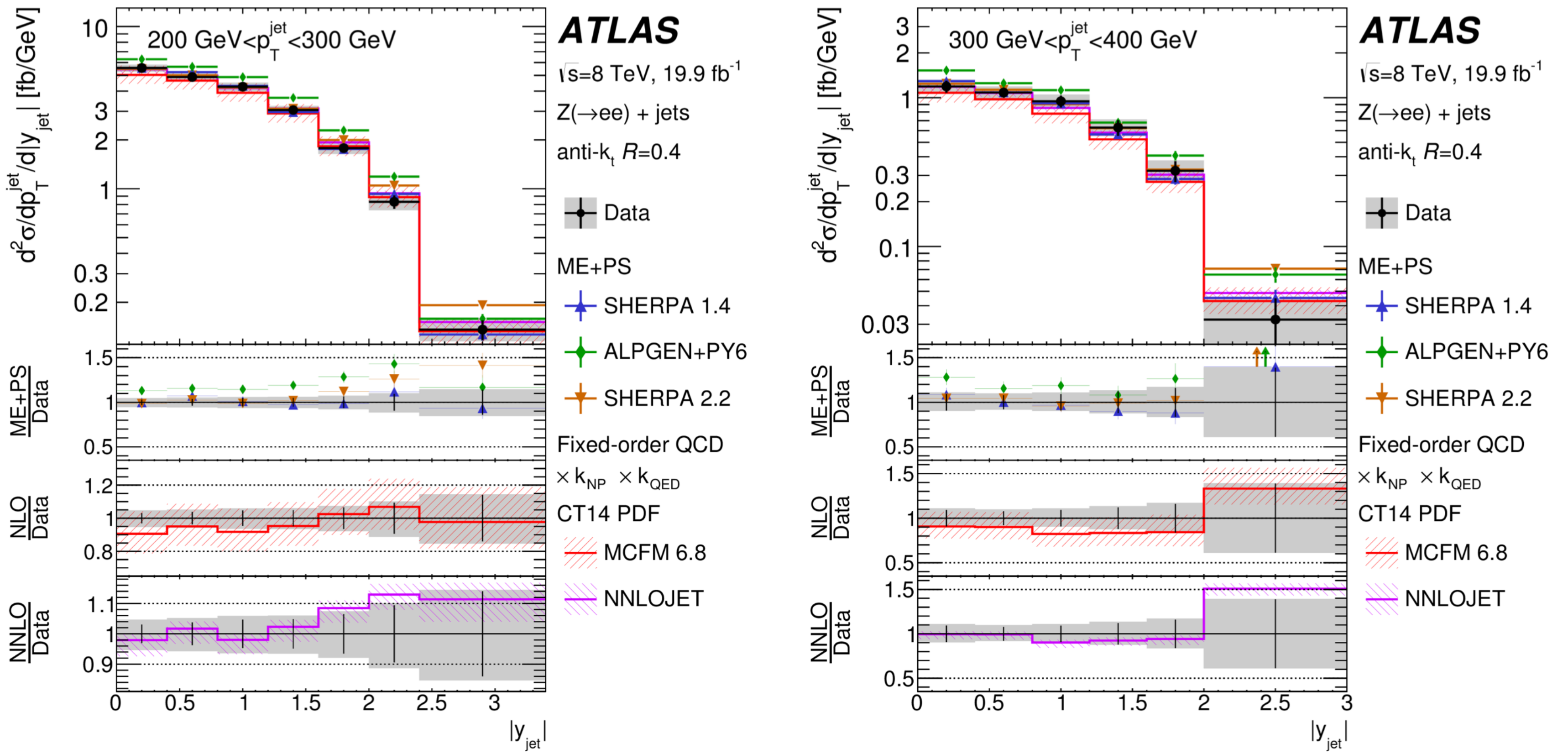

Eur. Phys. J. C 79 (2019) 847

Z + jets cross-section at 8 TeV

- NLO predictions calculated with various PDF sets / Measured cross-sections

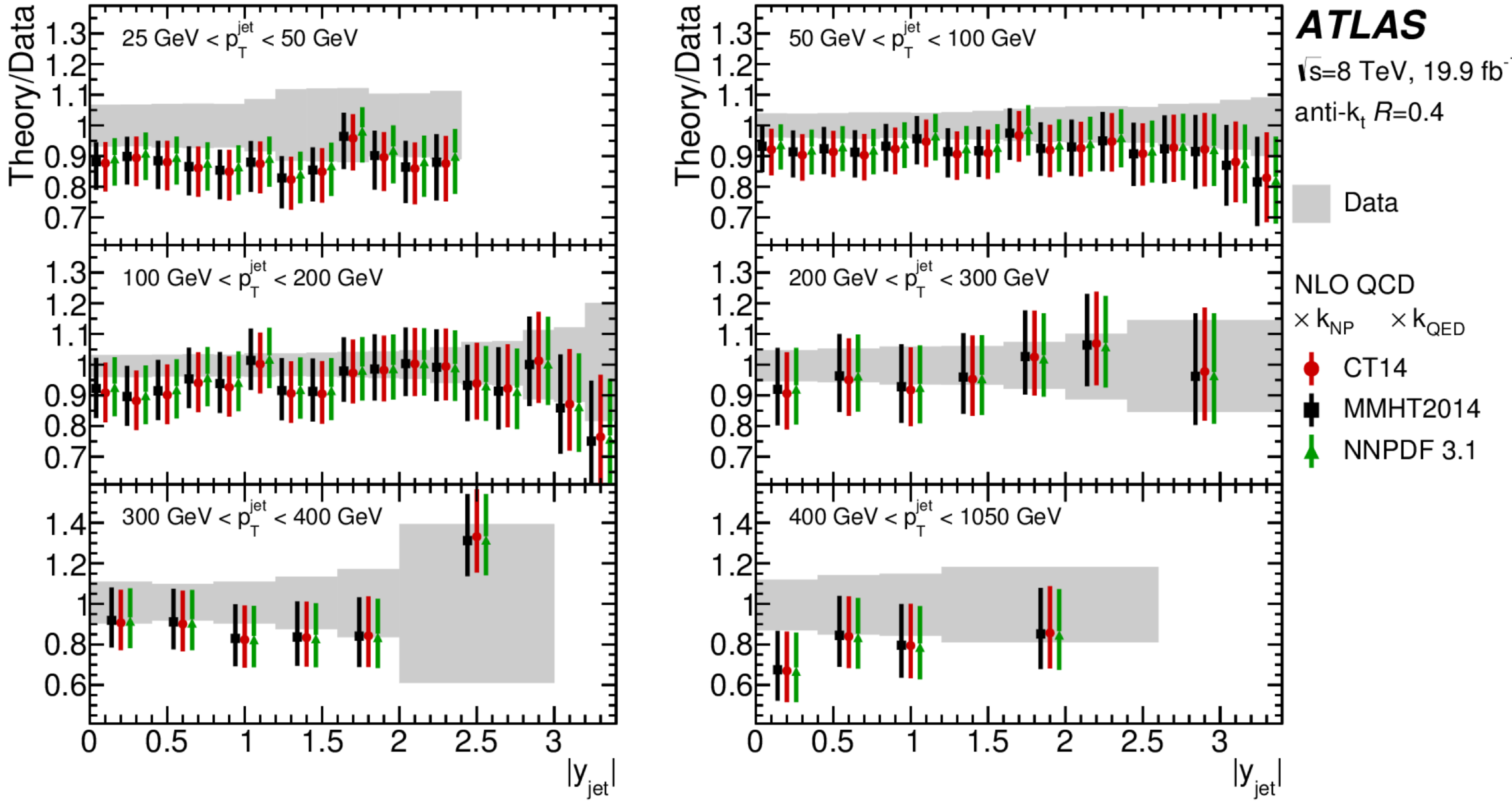

- NLO predictions with CT14, MMHT2014 and NNPDF PDF sets are in agreement within corresponding PDF uncertainties

Z + jets cross-section at 8 TeV

- Measured cross-sections / NLO predictions, calculated with various PDF sets

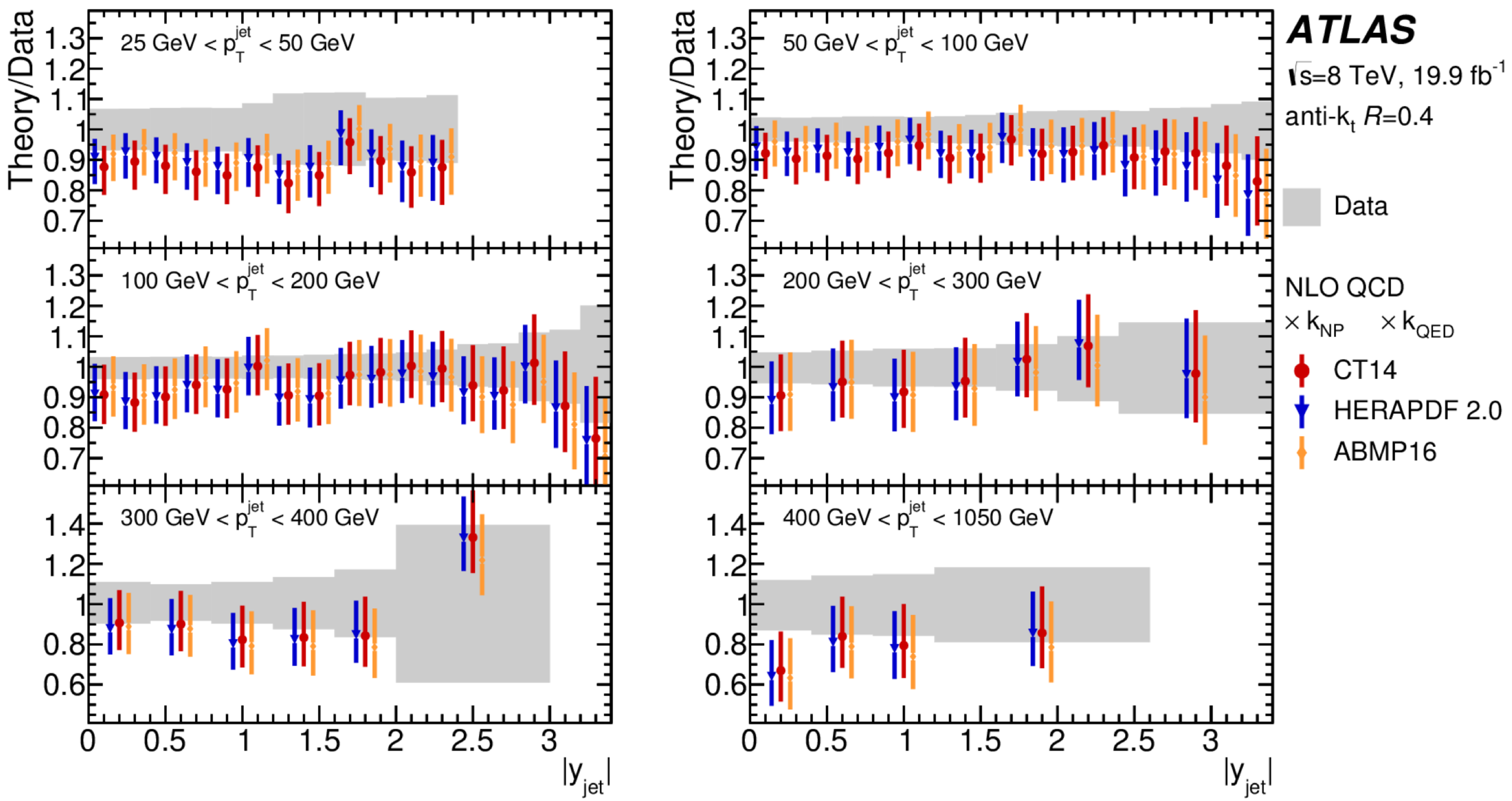

- Differences between the cross-sections calculated at NLO accuracy with various PDF sets are covered by the theoretical uncertainties

Z + jets cross-section at 8 TeV

- Measured cross-sections / NLO predictions, calculated with various PDF sets

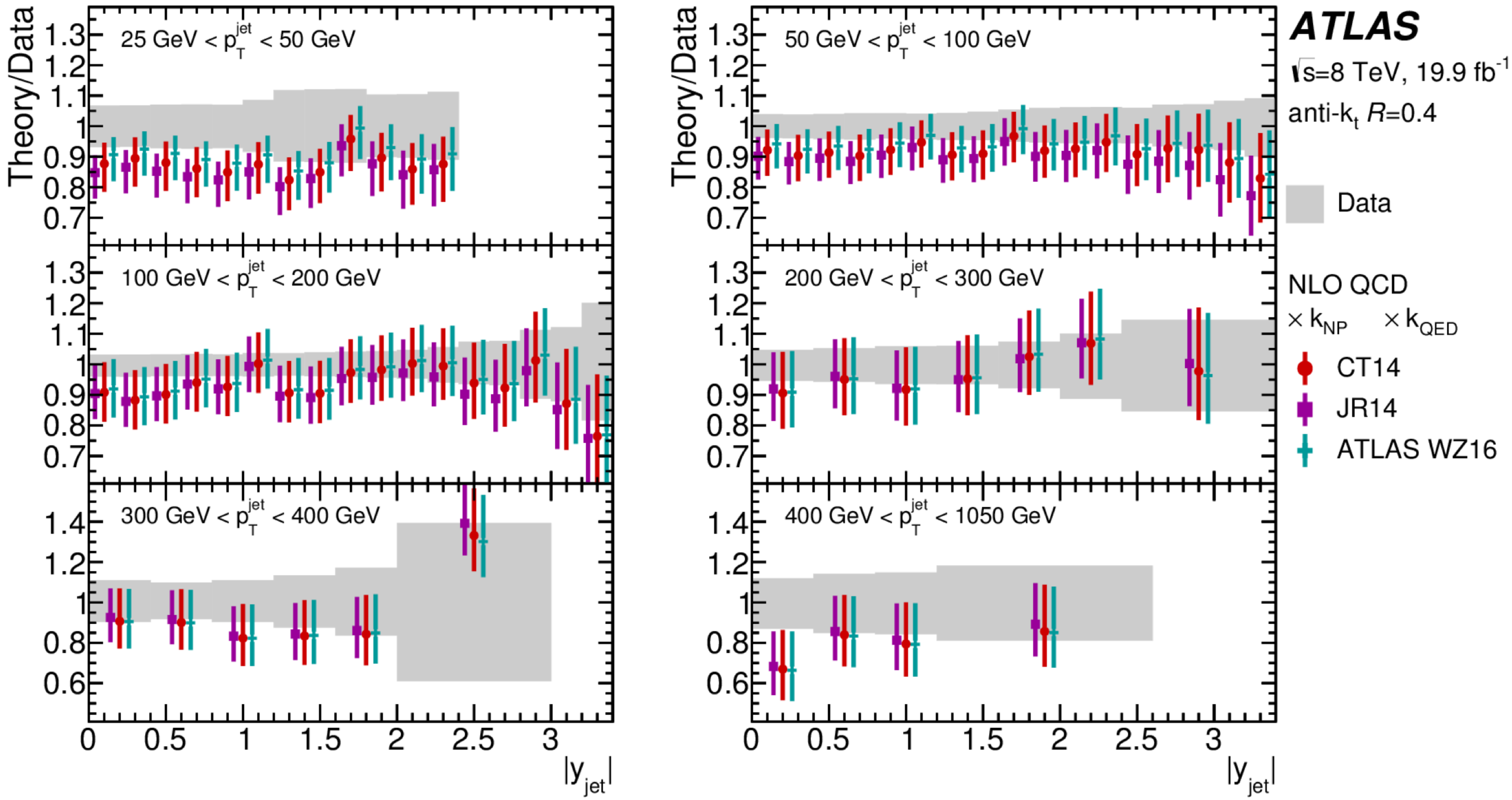

- Differences between the cross-sections calculated at NLO accuracy with various PDF sets are covered by the theoretical uncertainties

Z + jets cross-section at 8 TeV

- Measured cross-sections / NNLO predictions, calculated with various PDF sets

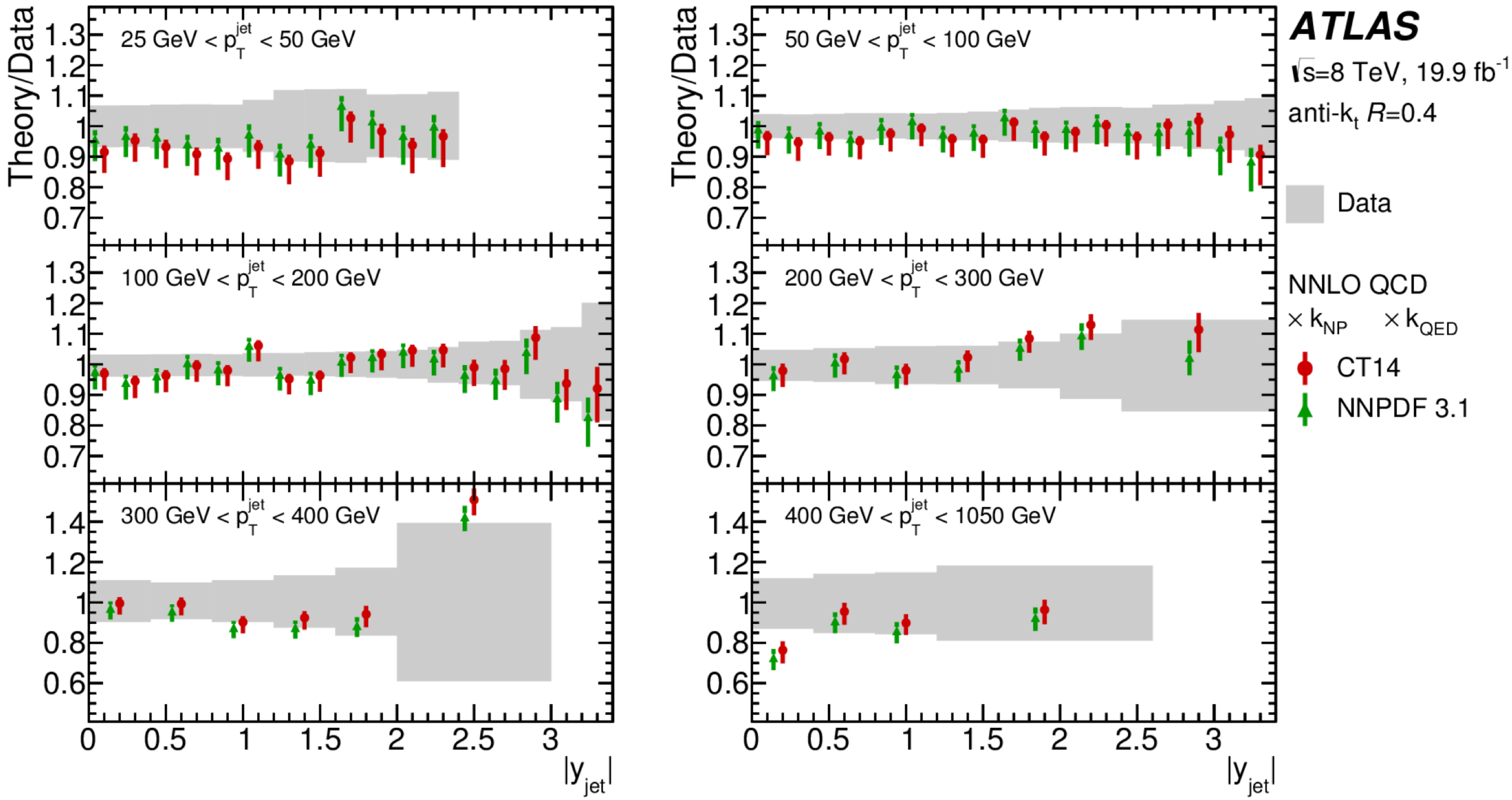

- Differences between the cross-sections calculated at NNLO accuracy with various PDF sets are covered by the theoretical uncertainties

Z + jets cross-section at 8 TeV

	p_T^{jet} range [GeV]	CT14nlo	CT14	NNPDF3.1	MMHT2014	ABMP16
			$p_T^{jet} > 25$ GeV			
χ^2_{uncorr}	$25 < p_T^{jet} < 50$	38.9	40.5	42.3	41.3	38.7
	$50 < p_T^{jet} < 100$	32.1	33.0	37.5	39.2	31.6
	$100 < p_T^{jet} < 200$	26.4	27.8	31.0	31.7	27.8
	$200 < p_T^{jet} < 300$	6.3	6.3	5.1	5.6	4.1
	$300 < p_T^{jet} < 400$	2.9	3.0	2.9	3.1	2.5
	$400 < p_T^{jet} < 1050$	2.2	2.4	2.2	2.3	1.7
χ^2_{corr}		21.2	19.8	19.3	18.7	17.8
χ^2/n_{bins}		129.9/63	132.6/63	140.0/63	141.9/63	124.3/63
			$p_T^{jet} > 50$ GeV			
χ^2_{uncorr}	$50 < p_T^{jet} < 100$	24.4	24.8	26.9	27.1	24.8
	$100 < p_T^{jet} < 200$	24.4	24.6	26.6	27.7	22.7
	$200 < p_T^{jet} < 300$	4.4	4.2	4.4	4.7	3.4
	$300 < p_T^{jet} < 400$	2.7	2.8	3.0	3.1	2.5
	$400 < p_T^{jet} < 1050$	3.6	4.0	3.8	3.9	2.9
χ^2_{corr}		6.5	4.7	4.3	5.1	4.1
χ^2/n_{bins}		66.1/51	65.2/51	69.0/51	71.6/51	60.4/51
			$p_T^{jet} > 100$ GeV			
χ^2_{uncorr}	$100 < p_T^{jet} < 200$	24.8	25.0	25.9	26.6	22.4
	$200 < p_T^{jet} < 300$	3.2	3.3	4.1	4.4	3.3
	$300 < p_T^{jet} < 400$	2.7	2.8	3.0	3.1	2.6
	$400 < p_T^{jet} < 1050$	3.4	3.8	3.6	3.6	3.3
χ^2_{corr}		4.9	3.7	2.7	4.1	2.3
χ^2/n_{bins}		39.0/34	38.5/34	39.3/34	41.8/34	33.8/34

- Very good agreement is observed when using $p_T^{jet} > 50$ GeV bins
- Not so good agreement is observed when $25 < p_T^{jet} < 50$ GeV bin is included in the global fit